

AMERICAN UNIVERSITY OF BEIRUT

THE EFFECTS OF GLYCOSAMINOGLYCANS
SULFATION ON LUNG CANCER CELLS GROWTH IN
3D *IN VITRO* MODELS

by

NADA MOHSEN ALMATARI

A thesis
submitted in partial fulfillment of the requirements
for the degree of Master of Science
to the Department of Biomedical Engineering
of the Maroun Samaan Faculty of Architecture and Engineering and Faculty of
Medicine
at the American University of Beirut

Beirut, Lebanon
February 2020

AMERICAN UNIVERSITY OF BEIRUT

THE EFFECTS OF GLYCOSAMINOGLYCANS
SULFATION ON LUNG CANCER CELLS GROWTH IN
3D *IN VITRO* MODELS

by
NADA MOHSEN ALMATARI

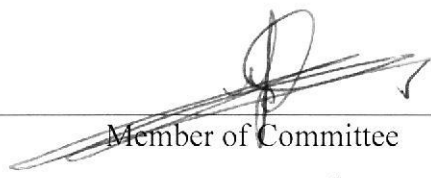
Approved by:

Dr. Rami Mhanna, Assistant Professor
Department of Biomedical Engineering



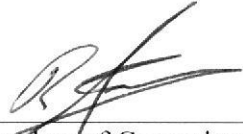
Advisor

Dr. Massoud Khraiche, Assistant Professor
Department of Biomedical Engineering




Member of Committee

Dr. Rabih Talhouk, Professor
Department of Biology



Member of Committee

Dr. Wassim Abou Kheir, Associate Professor
Department of Anatomy, Cell Biology, and Physiological Sciences



Member of Committee

Date of thesis defense: February 13, 2020

AMERICAN UNIVERSITY OF BEIRUT

THESIS, DISSERTATION, PROJECT RELEASE FORM

Student Name: ALMATARI NADA MOHSEN
Last First Middle

Master's Thesis Master's Project Doctoral Dissertation

I authorize the American University of Beirut to: (a) reproduce hard or electronic copies of my thesis, dissertation, or project; (b) include such copies in the archives and digital repositories of the University; and (c) make freely available such copies to third parties for research or educational purposes.

I authorize the American University of Beirut, to: (a) reproduce hard or electronic copies of it; (b) include such copies in the archives and digital repositories of the University; and (c) make freely available such copies to third parties for research or educational purposes after:

- One ---- year from the date of submission of my thesis, dissertation, or project.
- Two ---- years from the date of submission of my thesis, dissertation, or project.
- Three ~~---~~ years from the date of submission of my thesis, dissertation, or project.

 21-2-2020
Signature Date

ACKNOWLEDGMENTS

I could never have reached the heights or explored the depth without the help, guidance, support, and efforts of a lot of people.

First, I would like to thank my advisor Dr. Rami Mhanna, I am hugely indebted to you for showing me always interest in my research, and for giving me a lot of advice.

I would like to thank my mentor and supporter Dr. Wassim Abou Kheir for giving me the chance to do most of my experiments in his lab, teaching me the qualities of being a scientist and being there to answer all my question. Also, I would like also to thank my committee members, Dr. Massoud Khraiche and Dr. Rabih Talhouk and I am pretty grateful for your comments and kind words. Also, I would like to thank Dr. Humam Kadara, who believed in my abilities, gave me the chance to start the experimental works in his lab, and provided me with the most materials I used them throughout my journey.

A very special thank you goes to George Deeb, my partner in crime, who helped me a lot throughout my thesis. I wish you all the best in your Ph.D. and future.

A very special thank you goes to Dr. Abou Kheir's lab members, the WAKers, especially Jolie, Hiba, Joyce and Amani for their friendly attitude and support. They have lent me overall this year. Also, I would like to thank Dr. Kadar's Lab members and Dr. Mhanna's lab Members.

Thanks also go out to my parents, my siblings, my uncle Abo Ali, his wife, and my friends Reem and Hiba Zeid who keep praying for me and giving me continuous encouragement throughout my study.

I would like to express my special thanks to my beloved and supportive husband who is always by my side when times I needed him most and helped me a lot in finishing this study.

Above all, greatest appreciation to the Almighty God who has given me the health and strength to finish this work, and without his graces and blessings, I would never have been reached into this level.

Thanks a lot for everyone.

AN ABSTRACT OF THE THESIS OF

Nada Mohsen AlMatari

for

Master of Science

Major: Biomedical Engineering

Title: The Effects of Glycosaminoglycans Sulfation on Lung Cancer Cells Growth in 3D *in vitro* Models

Despite the recent research and medical advances, non-small cell lung cancer (NSCLC) remains the most diagnosed lung cancer subtype and the leading cause of cancer-related deaths. Lung adenocarcinoma (LUAD) is the most common NSCLC subtype with KRAS, GTPase, being the most frequent oncogene. KRAS-mutant LUAD is very aggressive, invasive, and resistant to most of the therapies, including chemotherapy. Cancer development strongly relies on cell proliferation and migration, which in turn requires an interaction with the extracellular matrix (ECM). The ECM is mainly composed of proteins and glycosaminoglycans (GAGs), which maintain tissue structure and regulate cell function. GAGs are known to modulate cellular functions mainly through their interactions with cytokines and growth factors (GFs). Particularly, sulfated GAGs, such as heparin, have been shown to enhance the binding of GFs and angiogenesis mainly by altering their sulfation patterns. In the current work, we assessed the effect of the sulfation of heparin-mimetic sulfated GAGs on the proliferative and tumorigenic characteristics of KRAS-mutant LUAD cells. Sulfated alginates (SulfAlg) shown earlier to have heparin-mimetic properties were synthesized with varying degrees of sulfation (DS=0, 0.8, 2.0 and 2.7) and their effects on KRAS-mutant LUAD cells were assessed using two-dimensional (2D) and three-dimensional (3D) culture systems. The effects of SulfAlg were studied on two KRAS-mutant cell lines, H1792 and MDA-F471, derived from human and murine respectively. The increase in the DS of mimetic GAGs had insignificant effects on the proliferation of H1792 grown in 2D, using MTT and trypan blue exclusion assays. The proliferation of MDA-F471 unlike H1792 cells grown in 2D significantly decreased with the increase in the DS of SulfAlg for the highest dose of polysaccharides (100 µg/mL) used as shown by trypan blue exclusion assay, but insignificant decrease using MTT assay at the two different concentrations. Moreover, the migratory abilities of H1792 and MDA-F471 decreased significantly with the increase in the DS ($p < 0.001$), as shown by the wound healing assay. The increase in the DS significantly decreased the sphere formation unit and the area of spheres for both cell lines ($p < 0.001$). In conclusion, the increase in the DS of heparin-mimetic SulfAlg reduces the proliferation, migration and the area of spheres for KRAS-mutant LUAD *in vitro* possibly by differential binding to GFs. SulfAlg may be suitable for applications in cancer therapy after further *in vivo* validation.

CONTENTS

ACKNOWLEDGEMENTS.....	v
ABSTRACT.....	vi
LIST OF ILLUSTRATIONS.....	x
LIST OF TABLES.....	xii
LIST OF ABBREVIATIONS.....	xiii

Chapter

I. INTRODUCTION.....	1
A. Extracellular matrix.....	1
B. Glycosaminoglycans.....	2
1. Overview.....	2
2. Heparin.....	4
a. Overview.....	4
b. Role of heparin.....	6
C. Sulfated alginate as biomimetic sulfated GAGs.....	11
1. Alginates.....	11
a. Background.....	11
b. Uses of alginate in medical applications.....	13
2. Sulfated alginate.....	14
a. Chemical sulfation of alginate to form sulfated alginate.....	14
b. Properties of sulfated alginate.....	16
D. Lung cancer.....	20
1. Overview.....	20
2. KRAS-mutant lung adenocarcinoma.....	21

a. Overview.....	21
b. Cell origin of <i>KRAS</i> -mutant lung adenocarcinoma.....	23
2. Lung cancer stem cells.....	25
a. Background.....	25
b. Cell surface markers of lung cancer stem cells.....	26
c. Signaling pathways in lung cancer stem cells.....	28
E. Aims of the study.....	29
II. METHODOLOGY.....	31
A. Cell lines	31
1. Selection.....	31
2. Cell culture.....	31
B. Cell-viability/ trypan blue exclusion assay.....	32
C. Cell growth assay/ MTT.....	33
D. Wound-healing/scratch assay.....	34
E. Sphere formation assay.....	35
1. Seeding.....	35
2. Propagation.....	36
F. Total RNA extraction	37
G. Two-Step Quantitative Real-Time Polymerase Chain Reaction (qRT-PCR)	38
1. Reverse transcription of RNA to cDNA.....	38
2. Quantitative real-time PCR(qRT-PCR).....	39
H. Statistical Analysis.....	41
III. RESULTS.....	42
A. Effect of increase in DS of alginates at two concentrations on the proliferation of human and murine LUAD cells using MTT assay <i>in</i> <i>vitro</i>	42

B. The effect of different DS of alginates <i>in vitro</i> on the cell viability of LUAD cells.....	46
C. The increase in the DS of alginates inhibits the migration of H1792 and MDA-F471 <i>in vitro</i>	48
D. The increase in the DS of alginates reduces the sphere formation capacity in murine and human LUAD cells.....	55
1. Effect of increase in DS on the sphere formation unit (SFU).....	55
2. Effect of increase in DS on the area of a formed sphere (μm^2)...	56
E. The expression of some genes in human KRAS- mutant and murine	59
1. Effects of increase in the DS of alginates on the expression of some genes in human <i>KRAS</i> -mutant LUAD cells.....	59
2. Effects of increase in the DS of alginates on the expression of some genes in human <i>KRAS</i> -mutant LUAD cells.....	62
IV. DISCUSSION.....	65
BIBLIOGRAPGHY.....	71

ILLUSTRATIONS

Figure		Page
1.	Schematic structure of GAGs.....	3
2.	The most common structure of heparin sulfate is made up of IdoA2S-GlcNS6S.....	5
3.	Chemical structure of G block, M block and GM block in alginate	12
4.	Schema of alginate extraction from algae.....	12
5.	Various methods of chemical sulfation of alginates using different reagents.....	15
6.	Incidence of known mutations in adenocarcinomas of the lung.....	22
7.	The effect of different DS of alginates on the number of live H1792 and MDA-F471 at the two concentrations (10µg/ml & 100µg/ml).....	43
8.	The effect of the increase in the DS of mimetic GAGs on the morphology of H1792 and MDA-F471 cells.....	45
9.	The effect of different DS of alginates on the total number of RWPE1 at the two concentrations (10µg/ml & 100µg/ml).....	46
10.	The effect of different DS of sulfated alginates at the two concentrations (10µg/ml and 100µg/ml) on H1792 and MDA-F471 cells' proliferation using MTT assay.....	47
11.	Representative images of H1792 cells showing the effect of the increase in sulfation of alginates on cell migration	51
12.	Representative images of MDA-F471 showing the effect of the increase of DS of alginates on cell migration.....	53
13.	The increase in the sulfation of GAGs reduces the migratory potentials of human and murine KRAS-mutant LUAD cells.....	54
14.	Effect of increase in DS of alginates on SFU of H1792 and MDA-F471.....	56
15.	The effect of the increase in DS of alginates on the area of the spheres formed of both human and murine LUAD cells.....	57
16.	Diameters of H1792 spheres after treatment G2 spheres with different DS of alginates.....	58

17.	Diameters of MDA-F471 spheres after treatment G2 spheres with different DS of alginates.....	59
18.	Differential expression of selected stemness markers in H1792 spheres by qRT-PCR.....	61
19.	Differential expression of selected stemness markers in MDA-F471 spheres by qRT-PCR.....	64

TABLES

Table		Page
1.	Primer sequences and annealing temperature of some selected human genes.....	40
2.	Primer sequences and annealing temperature of some selected murine genes.....	41
3.	Thermal cycling conditions of qRT-PCR.....	41

ABBREVIATIONS

2D: two-dimensional

3D: three-dimensional

ALCAM: activated leukocyte cell adhesion molecules

ALDH: aldehyde hydrogenase

ALK: anaplastic lymphoma kinase

AT: antithrombin

AT1: alveolar type 1

AT2: alveolar type 2

ATF3: activating transcription factor 3

BASC: bronchioalveolar stem cell

CC10: clara-cell specific 10-KD protein

CCL20: chemokine (C-C motif) ligand 20

CS: chondroitin sulfate

CSC: cancer stem cell

CXCL: C-X-C motif chemokine

DMEM: Dulbecco's modified eagle media

DS: degree of sulfation

ECM: extracellular matrix

EGF: epithelial growth factor

EGFR: epithelial growth factor receptor

FBS: fetal bovine serum

FGF: fibroblast growth factor

FTIR: Fourier-transform infrared spectroscopy

G1: first generation

G2: second generation

GAG: glycosaminoglycan

Gal: galactose

GAPDH: glyceraldehyde 3-phosphate dehydrogenase

GDL: glucono- δ -lactone

GF: growth factor

GlcNAc: N-acetyl-D-glucosamine

GlucA: β -D-glucuronic acid

HA: hyaluronic acid

HClSO₃: chlorosulfonic acid

HGF: hepatocyte growth factor

HIT: heparin-induced thrombosis

HL: heparin-lithocholic acid

HH: hedgehog

HS: heparan sulfate

IdoA: iduronic acid

IL: interleukin

KRAS: Kirsten rat sarcoma viral oncogene homolog

KS: keratan sulfate

KSFM: keratinocyte serum-free media

LMWH: low molecular weight heparin

LUAD: lung adenocarcinoma

MS: mass spectroscopy

MTT: 3-(4, 5- dimethylthiazol-2-yl)-2, 5-diphenyltetrazolium bromide

NMR: nuclear magnetic resonance

NNK: nicotine-derived nitrosamine ketone

NSCLC: non-small cell lung cancer

PBS: phosphate-buffered saline

PG: proteoglycan

SCLC: small cell lung cancer

SFU: sphere-forming unit

SO₃: Sulfur trioxide

SP: side population

SulfAlg: Sulfated alginates

TBA: Tetrabutylammonium

TBP: TATA-box binding protein

TNF: tumor necrosis factor

TP53: tumor protein 53

UFH: unfractionated heparin

VEGF: vascular endothelial growth factor

Xyl: xylose

CHAPTER I

INTRODUCTION

A. Extracellular matrix

Tissues are made up of cells and a surrounding dynamic structure termed the extracellular matrix (ECM). The ECM is made up of various non-cellular macromolecular components, such as collagen, elastin, fibronectin, laminin, proteoglycans (PGs), glycoproteins, which vary in a tissue-specific manner. The ECM not only provides the cells and tissues with the structural scaffold but also interacts with the cells and induces signals that regulate the behavior of the cells and tissues through cellular feedback loops. It plays an essential role in regulating growth, migration, differentiation, homeostasis, and morphogenesis (Frantz et al., 2010; Järveläinen et al., 2009). During development and wound healing, the cells in the tissues remodel the ECM, because ECM is subjected to many enzymes, modifying proteins, tension, and post-translational modification (Daley et al., 2008). Moreover, ECM supports the organs, such as lungs by a strong and expandable three-dimensional (3D) mechanical structure producing effective tensile and compressive strength and elasticity. This structure regulates the functionality of lung cells by allowing the binding of growth factors, and the interaction with cell surface receptors (Pelosi et al., 2007). Investigators have provided several approaches to mimic the ECM and enable systematic studies on its role in the growth of cancer and normal cells, such as synthetic hydrogels, collagen coatings, and fibroblast treated plates (DeQuach et al., 2010). One of the common

practices used to mimic the ECM composition and dimensionality is the use of Matrigel™ coating which is a tumor-based tissue extract developed in 1972 at the Laboratory of Developmental Biology and Anomalies (LDBA). Currently, Matrigel™ is commercially available as a soluble and sterile fluid that gels at 37°C. Matrigel™ enables the growth of many cell types including differentiated cells taken from tissue explants, as it contains a wide variety of growth factors that supports cell growth. Matrigel™ is also suitable for tumor cell growth, as it enhances angiogenesis and prevents tumor cell apoptosis (Engbring & Kleinman, 2003; Kleinman & Martin, 2005).

B. Glycosaminoglycans

1. Overview

Glycosaminoglycans (GAGs) are a wide family of linear and long polysaccharides, found in most of the tissues with protein association. GAGs are made up of repeating disaccharide units with different degrees of acetylation and sulfation, types of bonding, and position of the glycosidic monomer composition. These disaccharides can be L-iduronic acid (IdoA), galactose (Gal), D-glucuronic acid (GluA), N-acetylglucosamine (GlcNAc), and N-acetylgalactosamine, with different lengths. GAGs consist of a wide range, including heparan sulfate (HS), heparin, chondroitin sulfate (CS), keratan sulfate (KS), hyaluronic acid (HA) and dermatan sulfate (Jackson, et al. 1991; Afratis, et al. 2012) (Figure 1). GAGs differ in their molecular mass, density, and biological activities. Thus, they are tissue-specific, and their functions depend on the demands of the tissues. Except for HA, all of them are sulfated GAGs and they are attached typically to transmembrane protein core via a serine residue

forming PGs. At the physiological pH, all the carboxylic acid and sulfate groups are deprotonated, making the GAGs with highly negative charge density, and with heparin having the highest negative charge density (Capila & Linhardt, 2002).

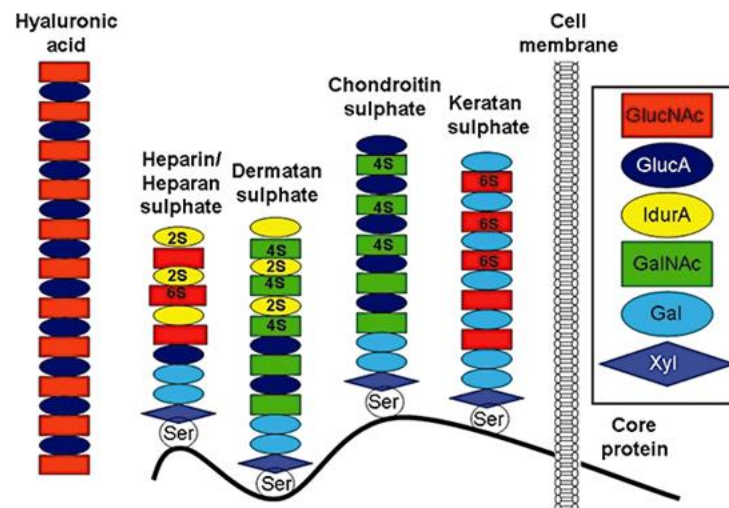


Figure 1: Schematic structure of GAGs. In the ECM, all GAGs, except HA are linked to transmembrane proteins through serine residues. GlucA, D-glucuronic acid; IdurA, L-iduronic acid; GalNAc, N-acetylgalactosamine; Gal, galactose; Xyl, xylose; Ser, serine; 2S,4S, 6S, the position of sulfate residue on the sugar unit. Adapted from (Papakonstantinou & Karakiulakis, 2009).

In general, GAGs act as protein receptors or activators, in which they are embedded directly in the ECM or function as integral parts of the ECM (R. L. Jackson et al., 1991; Papakonstantinou & Karakiulakis, 2009). GAGs have many important roles, such as homeostasis, development, angiogenesis, differentiation, cell adhesion, protein secretion, and gene transcription, by embedding membranal and nuclear processes. They bind selectively to various proteins and pathogens, which makes them the most important components in the ECM. Furthermore, GAGs undergo alteration and lead to many pathological conditions, such as inflammation, neurodegeneration, cancer, and infectious diseases. GAGs are the main component of ECM during embryonic development (Afratis et al., 2012; Derby, 1978; R. L. Jackson et al., 1991;

Papakonstantinou & Karakiulakis, 2009; Yung & Chan, 2007a). The roles of GAGs in lung diseases, as well as many other conditions, are not well studied mostly because of the heterogeneous distribution of native GAGs and the lack of biomimetic molecules that enable systematic investigations. However, the advanced techniques of purification, isolation, and characterization of GAGs have provided help in GAGs research. One of these ways is the use of dimethyl methylene blue assay for the quantification of sulfated glycosaminoglycans in tissue and fluid individual. Also, we can use the rapid spectrophotometric procedure to estimate the sulfated glycosaminoglycans in cartilage using the 1,9-dimethyl methylene blue dye at maximum absorption (R. Farndale et al., 1986; R. W. Farndale et al., 1982).

2. *Heparin*

a. Overview

Heparin is the most sulfated linear polysaccharides, consisting of repeating units of uronic acid in either its iduronic or glucuronic form, in which this domain is called S-domain with N- sulfated, attached to D-glucosamine residue, N-acetylated. It is mainly made up of alternating uronic acids, GlucA and GlcNAc, with the structure in Figure 2 represents about 60-85% of heparin in tissues (Carlsson & Kjellén, 2012; Sasisekharan & Venkataraman, 2000). Heparin is produced by mast cells; which line the blood vessels and mucosal membrane, and it is subjected to a series of enzymatic modifications in the Golgi apparatus, particularly by N-deacetylase-N-sulfotransferases, C-5 epimerases, and 2-O, 3-O and 6-O- sulfotransferase. These modifications lead to the heterogeneity of heparin in length, size, sulfation, and epimerization, mainly the

epimerization of GlucA into IdoA reveals flexibility in the heparin structure (Sasisekharan & Venkataraman, 2000). Their linkage region (-GlucA-Gal-Gal-Xyl-), which is made up of four monosaccharides, attaches to the core protein. Then, disaccharide GlucA and GlcNAc are added to the core protein. The addition of disaccharides is done by two glycosyl-transferases (EXT1 and EXT2), in which the GlcNAc's addition initiates the formation of CS, while the addition of GlucA will differentiate from CS and lead to the formation of HS/heparin chain (Carlsson & Kjellén, 2012). This complex process leads to the formation of a heterodimeric complex in the Golgi. Heparin has three sulfate groups, one attached to the 2-hydroxyl group of IdoA and the other two are linked to the 2-amino and 6-hydroxyl group of GlcNAc (Carlsson & Kjellén, 2012; Sasisekharan & Venkataraman, 2000) (Figure 2). Thus, heparin has high structural complexity due to the expression of tissue-specific isozymes.

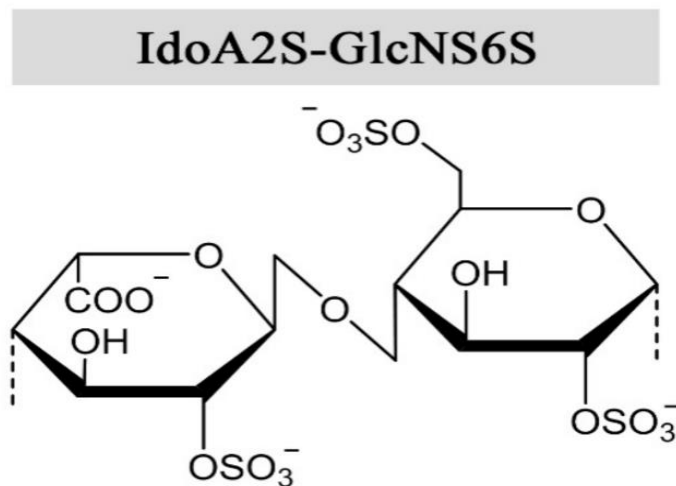


Figure 2:The most common structure of heparin sulfate is made up of IdoA2S-GlcNS6S. Adapted from (Øystein Arlov & Skjåk-Bræk, 2017).

b. Role of heparin

Heparin is different from other GAGs since it is produced by the mast cells and is secreted from the storage granules by exocytosis. During the synthesis of heparin, it is subjected to many enzymatic modifications that lead to wide biological activities. It has the highest degree of sulfation (DS) among GAGs and the highest charge density among biopolymers. As a result, it is associated with plenty of proteins, such as growth factors, adhesion proteins, disease-related proteins, and cytokines. Heparin binds selectively to the most important growth factors, such as fibroblast growth factors (FGF1 and FGF2). It interacts with the ECM to modulate cell signaling, thus enhancing the interference of the cells with their environments. Heparin plays a vital role in embryonic development, and pathological conditions, such as inflammation, wound healing, angiogenesis, and cancer. It interacts with many cellular molecules, such as chemokines, growth factors, morphogens, and enzymes. Also, it was found that heparin binds selectively to liver cells, in which it involves cell-cell adhesion. These interactions depend on the sequence of heparin, 3D structure, and binding sites (Øystein Arlov & Skj\aaak-Bræk, 2017; Capila & Linhardt, 2002; R. L. Jackson et al., 1991; Kjellén et al., 1977; Papakonstantinou & Karakiulakis, 2009; Sasisekharan & Venkataraman, 2000).

Through its N-terminal, heparin binds to and concentrates GFs in the surroundings of its cell-surface receptors, thus enhances angiogenesis or they can reduce angiogenesis by hindering the cellular diffusion of growth factors (Yung & Chan, 2007b). Heparin molecules have divergent structures that allow them to bind and regulate the activity of various growth factors by heparin-binding growth factors. For

example, it can bind to FGF indirectly through facilitating receptor dimerization, in which heparin binds multiple FGF molecules, and FGF binds tyrosine kinase receptors (FGFRs) and this leads to the activation of the receptor, or direct participation in receptor dimerization by binding to FGFRs. Thus, heparin stimulates the FGF-mediated signal transduction, in which FGF is important for angiogenesis, morphogenesis and wound healing (Faham et al., 1998). Moreover, heparin modulates tumor growth through the interaction with angiogenic growth factors, like FGF-10, or with anti-angiogenic antithrombin III (ATIII) (Sasisekharan & Venkataraman, 2000; Vivès et al., 1999). Also, hepatocyte growth factor (HGF) enhances the growth, morphogenesis, and motility of neural, epithelial and endothelial cells. Heparin binds to HGF's specific tyrosine kinase receptor MET, thus leads to the stimulation of roles of HGF (Birchmeier et al., 2003).

Heparin interacts with the ECM to modulate cell signaling, thus enhancing the interference of the cells with their environments. It regulates the vascular smooth muscle growth *in vivo*, in which it is predominant in non-regenerating vascular beds and diminishes in actively regenerating ones (Castellot et al., 1981). Heparin is stored in the mast cells and released into the vasculature at sites of tissue injury (Marcum et al., 1986). So, it has a role in immune defense against invading bacteria and foreign compounds. Mainly, heparin acts as an anticoagulant by binding to plasma protein ATIII and improving its inhibitory effect against serine proteases of the coagulation system. The activated ATIII, which is a glycoprotein of the heparin-binding site and high affinity to heparin, inhibits the binding of the pro-coagulation factors such as

thrombin to the Xa factor, thus reducing the coagulation. This anticoagulant effect is due to the allosteric activation of ATIII, by the interaction of the pentasaccharide chain of heparin that is very important to the anticoagulation effect. This pentasaccharide chain contains 3-O-glucosamine that is enough and necessary for the inhibition of the Xa factor. So, clinically heparin is used as an anticoagulant in thrombosis, but to allow this heparin chain to inhibit Xa factor, the commercial heparin should be of length more than 16 monosaccharides and the ratio of sulfate to carbon should be high to ensure the strong interaction between heparin and ATIII (Meer et al., 2017).

Moreover, heparin not only acts as an anticoagulant, but it also has many other important biological roles. Tumor cells need oxygen and nutrients to grow, so targeting the angiogenic factors that lead to the formation of new blood vessels will enhance antitumor effects by antiangiogenic effects. Heparin interferes in regulating the tumor growth, by forming a protective barrier of fibrin shell around the tumor and developing blood vessels that will support the immune system to fight the formed tumor. Also, it was found that heparin reduces the metastasis of lung carcinoma cells in mice (Hejna et al., 1999), pancreatic cancer and metastatic breast cancer (Zhang et al., 2016). So, heparin reduces the metastasis of cancerous cells rather than the primary tumor growth. Also, the study by Niu et al. showed the effect of low molecular weight heparin (LMWH) on reducing the chemo-resistance of cancer stem cell (CSC)-like lung adenocarcinoma cells by enhancing the ABCG2 protein degradation via the proteasome pathway, in which ABCG2 is a member of ATP binding cassette (ABC) transporter protein family, since this protein is very effective in protecting the cancer cells,

especially side population (SP), from chemo-resistant (Niu et al., 2012). Therefore, targeting CSCs will affect signaling pathways, such as Wnt, Hedgehog, and Notch pathways.

The studies about heparin and its structure have started in the 1920s. It was found that heparin can be extracted from animals, such as porcine mucosa or bovine lung, in which there are large quantities. Many studies were done to reach that the best animal source of heparin is porcine mucosa because it is cleaner and less degradable (Barrowcliffe, 2012). Heparin from porcine mucosa is the only animal heparin approved by the FDA, known as unfractionated heparin (UFH). UFH is used to produce more efficient heparin, low molecular weight heparin (LMWH), using chemical and enzymatic depolymerization. It was found that LMWH is more efficient than UFH since it has less effect on hemorrhage and can be taken by outpatient with no need to monitor, unlike UFH (Barrowcliffe, 2012). Heparin is very heterogeneous due to the different degrees of sulfation and epimerization, the origin of extraction, and molecular weight. So, heparin can be commercially manufactured leading to the formation of heparin's analogs with homogenous sulfation such as dextran, deltrane, and sodium pentosan polysulfate (Esquivel et al., 1982). These analogs, in addition to the extracted ones, have effective roles. LMWH, such as dalteparin, inhibits cell viability and induces the proliferation of lung cancer adenocarcinoma (LUAD) cells *in-vitro* (Chen et al., 2008). Clinically, industrial heparin molecules, such as UFH, LMWH, and warfarin, have anti-tumor effects, by enhancing the anticoagulation and thus inhibiting the metastatic cancerous cells (Lazo-Langner et al., 2007). Also, heparin is used in manufacturing

biocompatible and biodegradable anti-cancerous targeted nanoparticles. These nanoparticles are accumulated selectively in the tumor, due to the presence of the EGFR antibody targeted to EFGR, in which it increases with about 40-80% in some solid tumors (Peng et al., 2011).

To avoid the side effects of high heparin dosage, such as intense hemorrhage, osteoporosis, and HIT (heparin-induced thrombosis), scientists have found many heparin derivatives, such as carboxyl-reduced heparin, neo-heparin, and heparin-steroid conjugate, these inhibit metastasis, angiogenesis and tumor growth. Bile acylated heparin was proven to be very effective in decreasing tumor growth in mouse models for long term exposure. The modifying of heparin-lithocholic acid (HL) with cyclic RGD (Arg-Gly-Asp) leads to the yielding of RGD peptide conjugated HL (cRGD-HL). cRGD-HL has shown selective binding to the endothelial tumor cells because the RGD sequence will be identified by the $\alpha_v\beta_3$ integrin overexpressed by the endothelial tumor cells. Unlike other heparin derivatives, this one has anti-adhesion and anti-migration effects *in vitro* and *in vivo* (Park et al. 2008). Also, Hoppensteadt's study reported the role of heparin and its derivatives in the inhibition of tumor growth and angiogenesis, by downregulating vascular endothelial growth factor (VEGF) levels in mouse Lewis lung carcinoma model, a model with epidermoid lung carcinoma (Hoppensteadt et al., 2012). Sulfated GAGs using naturally extracted sulfated materials are challenging due to the heterogenic nature of native sulfated GAGS, and difficulty and high-cost of purifying sufficient quantities with homogenous DS. Therefore, we and others

developed biomimetic sulfated GAGs with controlled patterns (Fan et al., 2011a; Freeman et al., 2008b; Mhanna et al., 2017; Ronghua et al., 2003a).

C. Sulfated alginates as biomimetic sulfated GAGs

I. Alginates

a. Background

Alginate, a natural structural polysaccharide, is extracted from the cell walls of brown algae (*Phaeophyceae*), or the exocellular polysaccharides of gram-negative bacteria genera (*Azotobacter* and *Pseudomonas* species) with structural and protective activities (Øystein Arlov & Skjåk-Bræk, 2017; Rehm & Valla, 1997). Although they are not found in mammals, they still share some chemically structural properties with heparin. Alginates are linear copolymers, with blocks of (1,4)-linked β -D-mannuronate (M) and α -L-guluronate (G) residue. The M and G residues are C5 epimers like GlcA and IdoA in heparin. Alginate blocks are made up of repeated G residues (GGGGGG), repeated M molecules (MMMMMM), and alternated G and M molecules (GMGMGM), as shown in Figure 3 (Øystein Arlov & Skjåk-Bræk, 2017; Lee & Mooney, 2012; Rehm & Valla, 1997; Tønnesen & Karlsen, 2002). It was found that GM polymers give the alginates more opportunities to be used in biomedical engineering (Øystein Arlov & Skjåk-Bræk, 2017; Rehm & Valla, 1997). The molecular weight of alginates ranges from 32,000-400,000 g/mol. This variation of molecular weight leads to a wide spectrum of alginates' physical properties (Lee & Mooney, 2012).

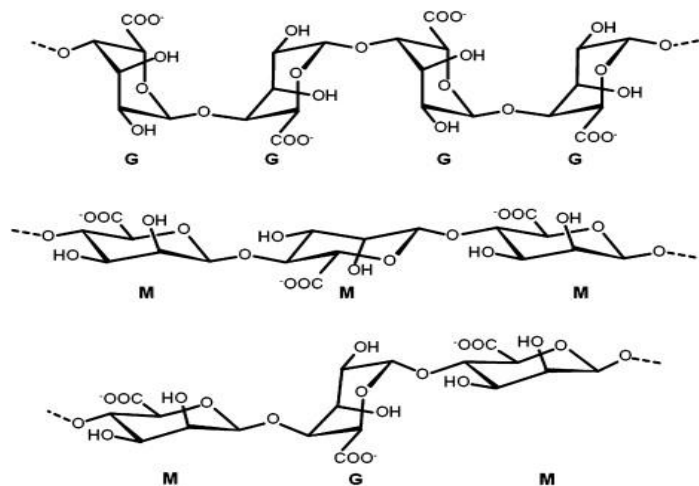


Figure 3: Chemical structure of G block, M block and GM block in alginate. Adapted from (Lee & Mooney, 2012).

Alginates are extracted from brown algae by the reaction with aqueous alkali solution like NaOH, to remove the protons attached to the alginates and form of alginic acid. Then, sodium chloride is added to neutralize and precipitate the formed alginate. After that, processes of transformation into alginic acid, purification, and conversion lead to the formation of water-soluble sodium alginate powder, as illustrated in Figure 4 (Pawar & Edgar, 2012).

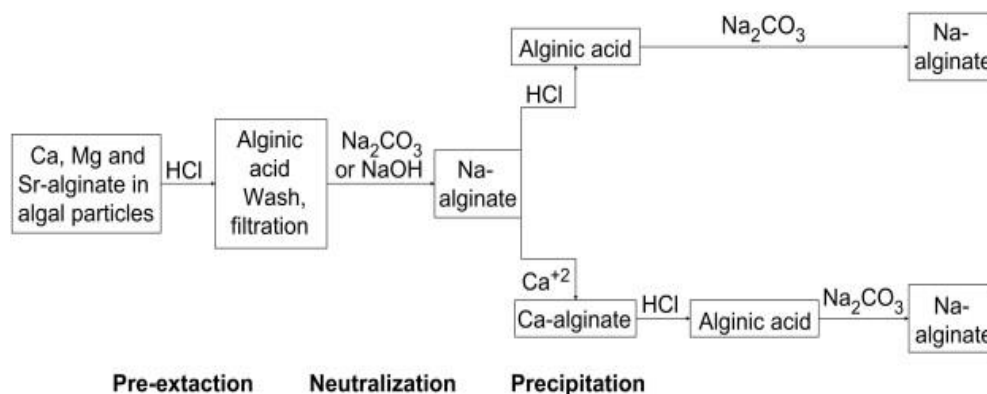


Figure 4: Schema of alginate extraction from algae. Adapted from (Pawar & Edgar, 2012).

b. Uses of alginate in medical applications

The bacterial source can give more chemically and physically defined alginate structures than alginate from seaweed, which is more promising in biomedical applications (Rehm & Valla, 1997), but the alginate from brown algae is more immunogenic, more abundant, and less cost. Sodium alginates are crossing-link with divalent cations, such as Ca^{2+} to enhance gelation (Pawar & Edgar, 2012; Tønnesen & Karlsen, 2002). Alginates have mechanical strength, gelation property, and cell affinity. These properties enable scientists to use alginate in scaffold implantation to support implanted tissues and organs. Also, alginates are inert and naturally biocompatible with cells and biomolecules, therefore they are used in many biomedical applications, such as transplantation of encapsulated cells which provides isolation and protection of the encapsulated cells from the attack of the immune system (Jacobs-Tulleneers-Thevissen et al., 2013). Alginates provide a slow-release matrix for drugs since they control the swelling release behavior of drugs and prevent their burst (Lee & Mooney, 2012; Tønnesen & Karlsen, 2002). Alginates are used in *in vitro* tissue engineering applications, which provide immune-isolation, mimic the ECM, serve as bio-ink in 3D-bioprinting (Markstedt et al., 2015), immobilize drugs for delivery system, and cells (Smidsrød & Skjåk-Bræk, 1990). Also, they act as an alginate wound dressing to reduce bacterial infection and enhance wound healing (Lee & Mooney, 2012). Alginate hydrogels transport cells to the targeted site and ensure space for newly formed tissue. It is used to form porous alginate beads that enhance the cell-invasion in tissue-engineered applications (Eiselt et al., 2000).

2. *Sulfated alginates*

a. Chemical sulfation of alginate to form sulfated alginate

The inertness of alginate does not affect the interactions with cell receptors and cell factors like GAGs. Also, the presence of carboxyl groups in each of its residues, and its composition of (1-4) linked β -D-mannuronate and α -L-guluronate residue makes alginates very close to GAGs, but they miss the presence of sulfated groups. As the result, the chemical sulfation of alginates acts to mimic GAGs by the presence of sulfated and carboxyl groups in the residues of the polysaccharides (Øystein Arlov & Skjåk-Bræk, 2017; Ronghua et al., 2003b). Sulfated alginates are produced via many chemical sulfation mechanisms of alginates. First, the reaction of chlorosulfonic acid (HClSO₃) in formamide, by Huang and co-workers, resulted in approximately 1.2 sulfated groups per monosaccharide. This mechanism leads to high sulfation, so to reduce the side effects of high sulfation, the sulfated alginates were conjugated with quaternary amines, thus reducing the over-sulfation and decreasing the anti-coagulant activity of sulfated alginates (Ronghua et al., 2003b). Changing the concentration of chlorosulfonic acid showed changing in the DS to reach a plateau between 1-1.2 (Øystein Arlov et al., 2015). Also, the use of sulfur trioxide (SO₃) in pyridine as a sulfation method for dextran showed better substitution than that of the HClSO₃/formamide method (Miyaji & Misaki, 1973). Consequently, Mhanna and co-workers used pyridine to produce sulfated alginates, but they enhance the solubility of alginates in pyridine by first the reaction of sodium alginate with tetrabutylammonium (TBA) bromide (Mhanna et al., 2013). The transformation of sodium alginates into TBA salt is followed by the substitution of the free hydroxyl groups with sulfated

groups using the sulfation method of $\text{SO}_3/\text{pyridine}$. This method can give sulfated alginate with different DS that is used in different experiments including the study of the effects of sulfated alginate hydrogels on the maintenance and proliferation of chondrocytes (Mhanna et al., 2013). Other mechanism uses a carbodiimide- H_2SO_4 intermediate reacting with sodium alginate directly (Ma et al., 2016) or TBA salt of alginate in DMF (Freeman et al., 2008). On the other hand, these two mechanisms depend on strong acids to obtain high DS, thus leading to partial depolymerization of high molecular weight alginate (Ma et al., 2016). Fan and co-workers stated the formation of sulfated alginate with 1.87 DS at optimal conditions using non-acidic sulfating reagent (Fan et al., 2011).

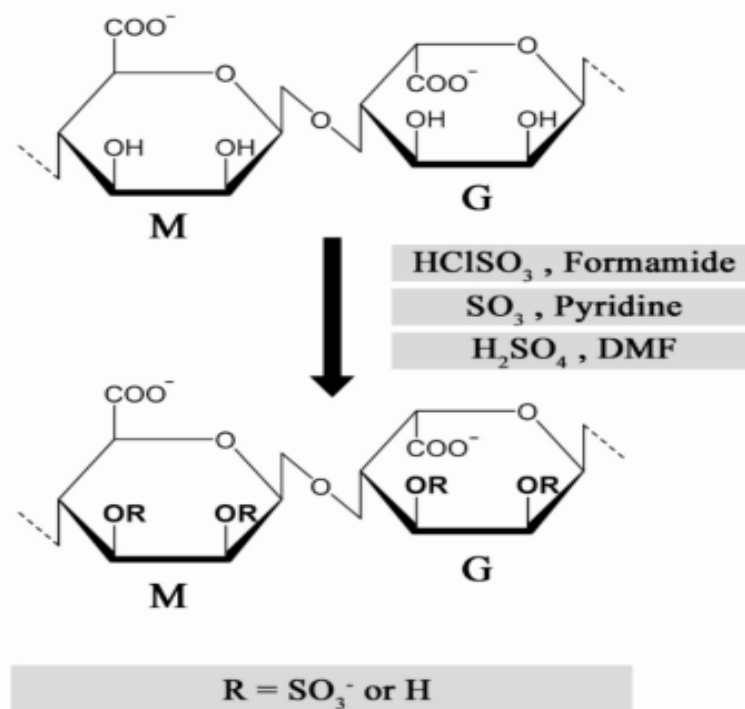


Figure 5: Various methods of chemical sulfation of alginates using different reagents. Adapted from (Øystein Arlov & Skjåk-Bræk, 2017).

The molecular structure of sulfated alginates has been detected by Fourier-transform infrared spectroscopy (FTIR), nuclear magnetic resonance (NMR) and mass spectroscopy (MS). The FTIR shows a peak representing the symmetric stretching of the S=O bond which is resulted from the sulfation of the hydroxyl groups of alginates. The NMR gives a lot of structural details, but the heterogeneity of the sulfated alginate leads to highly complex spectra. The chemical sulfation of alginate is less random substitution than the natural occurring heparin (Øystein Arlov & Skjåk-Bræk, 2017). The sulfated groups are distributed equally between C-2 and C-3 of mannuronic acid and guluronic acid units, resulting in a homogenous charge distribution along the chain (Fan et al., 2011). Mainly, this homogeneity can be provided by the formation of sulfated alginates using HClSO_3 . MS-based elementary analysis can be used to detect the degree of sulfation (DS) in sulfated alginates. DS is the average number of sulfates per one disaccharide repeating unit and it ranges from 0.0 (unsubstituted alginates) to 4.0 (fully substituted sulfation of all free hydroxyl groups of alginate) (Øystein Arlov & Skjåk-Bræk, 2017). There is consistency in the spectra of all the sulfated alginates formed by different mechanisms (Fan et al., 2011; Freeman et al., 2008; Mhanna et al., 2013; Ronghua et al., 2003), in which the IR (ATR, attenuated total reflectance): 3445, 2946, 1613, 1417, 1232, 1169, 1021, 951, 831, 796 cm^{-1} and C-NMR (D_2O): 178.1–177.6 (C 6), 102.3–101.8 (C-1), 80.9–69.9 (C-2, C-3, C-4), 66.3 ppm (C-5).

b. Properties of sulfated alginates

The chemical sulfation of alginates mainly affects the gelation property of alginates. It decreases the gelation of alginate hydrogels by reducing the stiffness and

increasing the swelling of alginates. Thus, the gelation decreases as the increase in the DS (Mhanna et al., 2014). However, the gelation capability of sulfated alginates can be maintained using enzymes to strengthen the gelation, or using CaCO₃- glucono- δ -lactone (GDL) crosslinking instead of CaCl₂ for controlled Ca²⁺ release, thus decreasing the gelation swelling (Øystein Arlov & Skjåk-Bræk, 2017).

It was proven that the chemical sulfation of alginates mimics the sulfated GAGs. Sulfated alginates give a promise for tissue engineering and drug delivery. They can act as heparin-analogous due to the similarities in their structures, in which the M and G blocks are C5 epimers like IdoA and GlcA of heparin. However, sulfated alginates do not turn-over rapidly as heparin molecules because our bodies as mammals do not possess the enzymes that break down the alginates.

Sulfated alginate acts as a cofactor of GFs and maintains their roles. Mhanna and co-workers have found that the proliferation and morphology of chondrocytes and expression of chondrocyte markers were promoted on sulfated alginate hydrogels (Mhanna et al., 2013). Also, sulfated alginates have the anticoagulant activity of the heparin through increasing the activated partial thrombosis time and not the activation of the AT factor (Fan et al., 2011; Ma et al., 2016; Ronghua et al., 2003). As a result, sulfated alginates have anticoagulant activity via sequestration and binding and/or inhibiting of protease activity of upregulated factors, but not through binding of sulfated alginates into anti-thrombin specifically. Moreover, they have anti-inflammatory effects that enhance the engineered tissues and reduce the host response of implanted biomaterials (Kerschenmeyer et al., 2017). Sulfated alginates are beneficial in osteoarthritis in which they inhibit cartilage damage by reducing oxidative stress and

inflammation. The increase in the DS of sulfated alginates leads to a decrease in the expression of pro-inflammatory markers in human chondrocytes, such as IL-6 and CXCL8. It is also found that sulfated alginates promote the macrophagic division, thus downregulate the gene expression of proinflammatory cytokine TNF- α (Kerschenmeyer et al., 2017). Likewise, sulfated alginate microspheres showed a lowering in inflammatory responses in the blood model by preventing the bursting of encapsulated cells and quarantining the cytokines in the hydrogel (Øystein Arlov et al., 2016). Then, they did another experiment to show that sulfated alginate hydrogels inhibit inflammation by sequestering of inflammatory cytokines and prevent the bursting of the encapsulated chondrocytes induced by inflammatory mediators IL-1 β in the hydrogels. Thus, sulfated alginates have anti-inflammatory and anti-catabolic properties that give more opportunities in tissue engineering and drug delivery (Ø Arlov et al., 2017). Freeman and coworkers showed that sulfated alginates promote the binding of heparin-binding peptides and proteins by mimicking the heparin-binding specificity (Freeman et al., 2008). Zhao and coworkers reported that sulfated alginates have efficacy in reducing the weight of granuloma in rats by inhibiting the inflammatory responses (Zhao et al., 2007).

Heparin was heavily used in tissue engineering and drug delivery, but its life span is small and turned over rapidly by the body. As a result, sulfated alginates give a promise for tissue engineering and drug delivery, because it was proven that the chemical sulfation of alginates mimics the sulfated GAGs. Sulfated alginates have anti-inflammatory effects that lead to enhance the engineered tissues and reduce the host response of implanted biomaterials (Kerschenmeyer et al., 2017). They bind the GFs

and have similar heparin-affinity to peptides and proteins (Freeman et al., 2008). Also, heparin-binding proteins bounded to sulfate alginate nanoparticles promoted repair of the tissues by releasing of the encapsulated GFs. These nanoparticles isolate the GFs from the proteases' activity (Ruvinov et al., 2016). Injectable sulfated alginates *in-vivo* showed affinity to bind to HFG. They enhance the biological roles of hepatocyte growth factor HGF, the controlled release of HFG, the infusion of the blood, and the angiogenesis in myocardial fracture model (Ruvinov et al., 2010).

Mhanna and coworkers showed that sulfated alginates enhance the phenotype of the cartilage, by increasing the expression of collagen I over collagen II. Sulfated alginates interact indirectly with integrin beta1, which maintains cell adhesion, proliferation, and migration. Thus, sulfated alginates allow the adhesion of the chondrocytes to the ECM by interacting with adhesion molecules (Mhanna et al., 2014). Also, the chondrogenic phenotype is sustained by the effects of sulfated alginates on the proliferation and phenotype of chondrocytes, Muller et. Al stated that sulfated alginates with nanocellulose fibers as 3D printing bio-inks maintain the proliferation, phenotype, and the formation of collagen II (Müller et al., 2017). Moreover, sulfated alginates influence angiogenic factors and enhance the formation of blood vessels. Freeman and Cohen showed that sulfated alginates scaffolds with bounding growth factors VEGF, TGF- β 1, and PDGF-BB implanted in the dorsal area of the rat enhance the formation of new blood vessels. The angiogenesis is maintained by the instantaneous release of angiogenic GFs bound to sulfated alginates in the scaffolds implanted, similar to the binding of these GFs to the heparin (Freeman & Cohen, 2009).

D. Lung cancer

1. Overview

Cancer is the leading cause of death worldwide with an estimated 9.6 million cancer-related deaths in 2018. It is caused by the changing of normal cells into tumor cells in a multistage process caused by genetic factors and/or external agents, such as physical carcinogens, chemical carcinogens, and biological carcinogens.

Approximately, 70% of cancer-related deaths occur in low- and middle- income countries. The most common types of cancer are lung, prostate, breast and colon cancer with about one-quarter of the cases in the USA are with lung cancer. Also, about 1.79 million deaths in 2017 and about 2 million new cases in 2018 are with lung cancer worldwide (Cheng et al., 2016; Siegel et al., 2019). Smoking leads to about 80% of lung cancer-related deaths. The survival rate of lung cancer cases is low and steady, due to the diagnosis at late stages (Siegel et al., 2019).

Lung cancer is categorized histologically into two types: non-small cell lung cancer (NSCLC) and small cell lung cancer (SCLC), with about 85% and 15% of all lung cancer cases, respectively (van Meerbeeck et al., 2011; Zappa & Mousa, 2016). NSCLC is categorized into three groups, squamous-cell carcinomas (SCC), lung adenocarcinomas (LUAD), and large-cell lung carcinomas. SCC derives from the epithelial cells of the airway bronchial tubes in the lung center. While LUAD derives from small bronchi, bronchioles or alveolar epithelial cells and is peripherally located. NSCLC is related neither to squamous nor to glandular maturation. It derives from the central part of the lung, near the lymph nodes, in the chest wall or other distant regions.

SCC and large cell carcinoma are associated mainly with smoking; however, LUAD is common in smokers and non-smokers (Zappa & Mousa, 2016).

2. *KRAS*-mutant lung adenocarcinoma

a. Overview

LUAD is divided into four categories: bronchioloalveolar, acinar, papillary, and solid. It represents around 40% of the NSCLC cases (Cheng et al., 2016) and about 50% of all lung cancer cases. LUAD is mediated molecularly by two common pathways.: an epithelial growth factor receptor (*EGFR*)- a dependent pathway and a Kirsten rat sarcoma viral oncogene homolog (*KRAS*) –signaling pathway(Figure 5) (Boolell et al., 2015a). The LUAD derived from smoker patients is mainly due to the alterations in the *KRAS* gene, whereas from the non-smoker patients are due to the *EGFR* and anaplastic lymphoma kinase (*ALK*) mutant genes (Kadara et al., 2012). Knowing the molecular alterations behind lung cancer helps to find potential targeted drugs. Also, it was recommended by the national guidelines to test for *EGFR*, *KRAS* and *ALK* for LUAD patients before starting any type of primary therapy (Lindeman et al., 2013), because *EGFR* and *KRAS* mutations are sensitive and resistant to the tyrosine kinase-inhibitor therapy respectively (Marks et al., 2008).

K-Ras belongs to a group of genes encoding membrane-bound low molecular GTP-binding protein, known as Ras-GTPase related family. K-Ras is activated by the binding of GTP that leads to the conformational changes and thus activation. After the activation, *KRAS* binds to several downstream signal transducers which upregulate several pathways, such as RAF-MEK-ERK-MAPK and PI3K-AKT-mTOR. These

pathways have essential roles in the proliferation, regulation, growth, and phenotype of the cells (Jančík et al., 2010). The activated form is switched to an inactive form by the hydrolysis of the GTP into GDP by the intrinsic GTPase activity of *KRAS* (Jančík et al., 2010). The *KRAS* mutations lead to amino-acid glycine substitution at positions 12 and 13. These mutations are one of the leading causes of lung, colon and pancreas cancer. They are the most common mutant oncogenes that lead to LUAD, with about 30% of all LUADs (Figure 6). Unlike *EGFR* mutations, *KRAS* mutations are associated with smoking etiology (Riely et al., 2009).

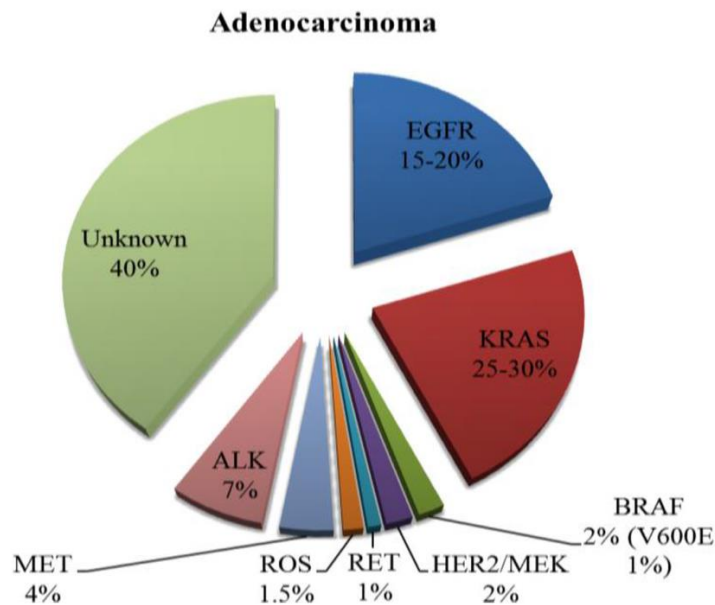


Figure 6: Incidence of known mutations in adenocarcinomas of the lung. Adapted from (Boolell et al., 2015).

The prognostic value of *KRAS* mutations has been studied for several years. Many trails have reported that most SCLC cases with *EGFR* mutations are sensitive to gefitinib, erlotinib and tyrosine kinase inhibitors. However, *KRAS* mutations that encode GTPase downstream of *EGFR*, have not shown any significant prognosis (Marks et al.,

2008). Also, *KRAS*-driven LUADs have resistance against chemotherapy, radiotherapy, and some targeted therapy (Marks et al., 2008; Meng et al., 2013). Consequently, it is very important to know the genomics behind the *KRAS*-driven LUAD to treated using molecular targeted therapy.

The heterogeneity of the *KRAS* mutation makes it very challenging to find effective and targeted therapy for *KRAS* or downstream effectors of the *KRAS* pathway (Sun et al., 2019). The overlapping of mutations in tumor suppressor *TP53* and *STK11/LKB1* is common in *KRAS*-driven LUADs, which leads to the complexity in *KRAS*-mutations with variation in gene expression, proliferation and immuno-response (F. Skoulidis et al., 2017; Sun et al., 2019). The mutation of tumor suppressor *TP53* occurs in about 30-50% of LUADs (Kadara et al., 2016) which leads to tumor growth and proliferation. Also, Liu et al. directed that *KRAS* mutant LUAD is mainly associated with smoking Sun et al, reported that *REG4* is overexpressed in *KRAS*- mutant LUADs, thus inhibiting of REG leads to the suppression of *KRAS* tumor growth (Sun et al., 2019). Moreover, there are additional gene alterations co-exited with *KRAS* to enhance the LUAD carcinogen, such as *ATM* and *KEAP1* that are involved in oxidative stress, cytoprotective signaling pathways, and DNA repair (Ferdinandos Skoulidis et al., 2015).

b. Cell origin of *KRAS*-mutant lung adenocarcinoma

The cellular components of the lungs vary along its proximodistal axis and contain a variety of epithelial cells. Thus, the lung can be divided into three main cellular compartments, the proximal conducting airway (bronchus), the distal bronchiolar epithelium, and the alveoli. The bronchus is made up of basal, ciliated,

secretory (Clara) and neuroendocrine cells. While the distal bronchiolar epithelium is made up of columnar non-ciliated club cells that are packed with many secretory granules and expressed glycoprotein secretoglobulin, known as Clara-cells specific 10KD protein (CC10) (Rock & Hogan, 2011). The third main compartment is the alveolar sacs, which are tiny thin-walled sacs and responsible for gas exchange. Alveolar epithelium, lining these sacs, is consisted of both type 1 (AT1) and type 2 (AT2) alveolar epithelial cells (Rock & Hogan, 2011).

The cellular origin of lung cancer is still controversial. The histologically different subtypes of lung cancer show that the cell origin or progenitors of lung cancer arise from distinct cells according to the subtype and the cellular components (Sutherland & Berns, 2010). LUAD is one of the most common subtypes of lung cancer. It is generally believed that LUAD is originated from the distal airway, mainly from the bronchioles, small bronchi, and alveolar epithelial cells (Sutherland & Berns, 2010). The cells of origin or progenitors of LUAD, which have stem-cell characteristics, was initially observed to be driven from the bronchioalveolar duct junction (BADJ), the site of the beginning of alveoli's formation (E. L. Jackson, 2001; Sutherland & Berns, 2010). Initially, Jackson et al. stated that a rare cell group co-expresses Clara cell marker, such as CC10, AT2 markers and surfactant protein C (SPC) (E. L. Jackson, 2001). Then, these observations stimulated Kim et al. to do the closest research on the type of this rare cell population, which leads to the expression of these markers in KRAS -mutant LUAD and this cell population, located in the BADJ, is named bronchioalveolar stem cells (BASC). BASCs, double-positive cells (CC10 and SPC), are dormant in normal cases, while they undergo proliferation and malignancy into club,

AT2 and AT1 cells in response to induced airway injury and their numbers increases with the increase in the size and the number of LAUD cells with codon 12K-Ras mutation (C. F. B. Kim et al., 2005). Later studies, Xu et. al tried to find the specific cell type capable of initiation of LUAD by reporting that Kras-mutant gene was induced in SPC-positive cells (BASCs and AT2 cells) and CC10-positive cells (club cells, BADJ cells, and a few AT2 cells) (X. Xu et al., 2012). They found that multiple cells proliferated due to *KRAS* induction, while only AT2 cells were able to initiate cancerous cells (X. Xu et al., 2012). Besides, more studies showed the essential role of AT2 cells in the initiation and development of *KRAS*- mutant LUAD (Mainardi et al., 2014; Sutherland et al., 2014). Recent studies by Fujimoto et al. reported that *Gprca*^{-/-} mutant mice developed LUAD from AT2 cells (Fujimoto et al., 2017).

3. Lung cancer stem cells

a. Background

Cancerous cells, like normal cells, are made up of heterogeneous cell populations that are reconstructed by a group of cells, with stem-like properties to self-renew and differentiate extensively into tumorous cells, named as cancer stem cells CSCs (Houghton et al., 2007). Targeting CSCs is one of the main aims of the new anti-cancer therapies, CSCs which are also known as tumor-initiating cells (TICs), might be responsible for the metastasis and relapse of cancer (Z. Yu et al., 2012).

In lung cancer, the CSCs were first discovered by Kim and his coworkers, in which they specified a population multipotent stem-cells named BASCs, in which these cells stimulated the proliferation and initiation of tumors in mice following K-Ras gene

activation (C. F. B. Kim et al., 2005). Then, it was identified by Eramo and his coworkers the lung CSCs which were isolated from histologically different lung cancer subtypes (Eramo et al., 2008). This lung CSCs are characterized by over-expression of cell surface marker CD133, extensive proliferation and self-renewal, under-expression of specific lineage markers, and ability to form tumors after xenotransplantation in mice (Eramo et al., 2008). Also, the lung CSCs were isolated as SP by Ho et al. from six different lung cancer cell lines with the ability to exclude Houchest 33324 dye, by the high expression of ATP-binding cassette family of transporter proteins in response to drug's resistance (Ho et al., 2007). These SPs have properties like stem cells, in which they show an increase in the ability of tumor-initiation, telomerase activity, and invasiveness (Ho et al., 2007). Until today, many studies isolated lung CSCs and identified them by using different surface cell markers and other cancer cell characteristics.

b. Cell surface markers of lung cancer stem cells

Several cell surface markers identify the characteristics of lung CSCs. CD44 is a surface marker that is essential for remodeling, cell-adhesion to ECM, cell-migration, and differentiation (Pine et al., 2008). The increase of CD44 expression stimulated the tumorigenic properties in NSCLC and mainly in LUAD cells than SCCs (Leung et al., 2010). CD44-expressed cells showed tumor -initiation, and high expressions of pluripotency genes, such as SOX2, NANOG, and OCT4 (Leung et al., 2010).

CD133 is a glycoprotein cell surface marker with undefined function, but it is found on the membrane of several CSCs (Pine et al., 2008). Eramo et al. showed that

CD133⁺ lung cancer cells have stem-like properties, in which they have higher tumorigenic abilities and differentiation into lung cancer cells (Eramo et al., 2008). On the other hand, other studies demonstrated that CD133⁻ cells have stem-like tumorigenic abilities, after xenotransplantation in mice, and CD133 is not associated with survival of patients with NSCLC (Salnikov et al., 2010). Thus, the role of CD133 in LUAD CSCs is still controversial, but the expression of CD133 is correlated with the chemotherapy resistance (Salnikov et al., 2010).

CD166 is another cell surface marker used to identify lung CSCs, known as activated leukocyte cell adhesion molecule (ALCAM) (Tachezy et al., 2014). It is a highly conserved glycoprotein from the immunoglobulin superfamily, and it is crucial in the development of various tissues, such as the upper airway. It was demonstrated that CD166 cell marker does not affect the tumorigenic ability of NSCLC since a study on NSCLC patients with CD166 expression showed no prognostic effect on the survival rate (Tachezy et al., 2014). Another study showed that the knocking down of CD166 in CSCs does not affect their tumorigenic abilities (Hardavella et al., 2016). Thus, CD166 is an inert cell surface marker, enriched NSCLC CSCs, but does not affect the tumorigenic activity (Hardavella et al., 2016).

Aldehyde hydrogenase (ALDH) superfamily is a group of cytosolic isozymes, that oxidize intracellular aldehydes, such as oxidizing of retinal into retinoid at the beginning of stem cells differentiation (Hardavella et al., 2016). It is a drug resistance gene present in most TICs, such as NSCLC cells, since it detoxifies many cytotoxic agents (Pine et al., 2008). High ALDH1 was shown to be associated with lung cancer cells with stem-like properties, like differentiation, self-renewal, and tumor-initiation

(Jiang et al., 2009). Also, it was proved that the expression of ALDH1 for 303 different specimens from lung cancer patients is associated with the stage and grade of lung cancer (Jiang et al., 2009). Moreover, ALDH1A1 and ALDH3A1 are overexpressed in epithelial lung CSCs from NSCLC patients than normal and SCLC cases (Hardavella et al., 2016; Pine et al., 2008). There are other NSCLC CSC's markers, including CD117, CD90, CD87, and polycomb ring finger oncogene (BMI-1) (Hardavella et al., 2016; Pine et al., 2008).

c. Signaling pathways in lung cancer stem cells

The behavior of the normal stem cells is controlled by signaling pathways, such as Notch, Hedgehog, and *Wnt* pathways. Thus, lung cancer can be due to errors in signaling pathways that lead to the uncontrolled proliferation of stem cells (Pine et al., 2008). To begin with, the Notch pathway is crucial in cell cycle progression and survival of lung stem cells. It determines the fate of epithelial cells in the proximodistal axis (Pine et al., 2008). The Notch pathway involves the maintenance of lung CSCs because it was found that in LUAD cells have high expression of notch pathway in the ALDH⁺ cells, enhanced self-renewal of NSCLC stem-like cells (Sullivan et al., 2010). The second one is the Hedgehog (HH) pathway, which is essential for the regulation of embryogenesis, such as Proliferation, Differentiation, and Migration of stem cells (Pine et al., 2008). The dysfunction of this pathway is mainly in SCC (Kwon-sik Park et al., 2011) and CD44⁺/ALDH⁺ CSCs (Liu et al., 2013). Therefore, the HH signaling pathway is important in the self-renewal and maintenance of CSCs. The third signaling pathway is *Wnt*/beta-catenin signaling, which is crucial for the embryogenesis and the

maintenance of pluripotency and differentiation of normal stem cells (Holland et al., 2013). It was proved that *Wnt* signaling cascades have a role in organogenesis and the formation of different functional tissues. This has raised the opportunity for *Wnt* signaling to be essential for self-renewal of not only stem cells but also CSCs. Thus, *Wnt* Signaling plays a crucial role in cancer development (Holland et al., 2013). Many studies reported the importance of *Wnt* signaling in lung cancer growth, in which it was stated that *Wnt* and *K-RasG12D* activation stimulate the development of lung tumor, proliferation of embryonic distal lung progenitor cells, and metastasis of lung cancerous cells (Pacheco-Pinedo et al., 2011). Therefore, these three signaling pathways are crucial in the development, growth, metastasis, and proliferation of lung tumors and CSCs and targeting these pathways has therapeutic and anti-cancer roles.

E. Aims of the study

According to what has been discussed before, LUAD is one of the most aggressive and lethal cancer subtypes. Also, it was found that sulfated alginates with high DS mimic heparin. Therefore, in our study we want to assess the effect of sulfated alginates with different DSs, mainly DS 2.0 and DS 2.7 on human and murine *KRAS*-mutant LUAD cells, H1792, and MDA-F471, respectively. To achieve this goal, we questioned the following aims:

- 1) To determine the effect of different DSs sulfated alginates on the growth and proliferation of H1792 and MDA-F471 in 2D culture using MTT and trypan blue assays.

- 2) To assess the effect of different DSs sulfated alginates on targeting LUAD CSCs using 3D sphere formation assay by analyzing the variation on the sphere formation unit and the area of spheres formed.
- 3) To evaluate the effect of different DSs sulfated alginates on different gene expression from the collected spheres

CHAPTER II

METHODOLOGY

A. Cell lines

1. Selection

The cell lines used in this study were the murine MDA-F471, the human H1792, and RWPE1. MDA-F471 was derived *de novo* from a LUAD that was formed in the lung of female *Gprc5a*^{-/-} mice sacrificed 16 months after exposure to the tobacco carcinogen NNK. The cells carry a G12D *KRAS* mutation, the same variant often observed in the human in human *KRAS*-mutant LUADs (Fujimoto et al., 2010). The human H1792 LUAD cell line was derived from the pleural effusion of a smoker 50-year-old Caucasian male with metastatic adenocarcinoma. H1792 cells exhibit a TP53 mutation in a splice donor site in addition to a G12C *KRAS* mutation (Sunaga, et al. 2011). The human RWPE1 cells, that are epithelial cells, are derived from the prostate of a 54-years-old normal Caucasian man.

2. Cell culture

MDA-F471 and H1792 cells were cultured in Dulbecco's Modified Eagle Media (DMEM) Ham's F-12 (Sigma Aldrich) supplemented with 10% heat-inactivated fetal bovine serum (FBS) (Sigma-Aldrich), 1 % penicillin-streptomycin antibiotics (Lonza), and 5 µg/ml Plasmocin™ Prophylactic (InvivoGen) for the prevention of mycoplasma contamination. While RWPE1 cells were cultured in keratinocyte serum-

free medium (KSFM) (GIBCO) supplemented with 0.004 % recombinant human epithelial growth factor (rhEGF). Cells were incubated in a humidified incubator (5 % CO₂) at 37°C. Typically, media was replenished every 2-3 days and when confluency of cells reached 70-80 %, cells were passaged. They were passaged by washing with 1X phosphate-buffered saline (PBS) (Lonza) followed by enzymatic dissociation using 0.05% trypsin-ethylene-diamine tetraacetic acid (EDTA) (Sigma-Aldrich) for 6 minutes (H1792 & RWPE1) or 12 minutes (MDA-F471) at 37°C. Subsequently, trypsin was neutralized by 1:1 complete growth medium. Cells were then centrifuged for 5 mins at 900 rpm and the supernatant was discarded. The pellet was resuspended in new fresh media and transferred into appropriate cell culture flasks. However, for RWPE1 the cell culture flask was coated with 1% collagen I with PBS for 15 mins before transferring the cells.

For the beginning of new experiments, cells were calculated using a hemacytometer on the four corner chambers, following this formula: cells/ml= average number of cells x dilution factor x volume of suspension (ml) x 10⁴. Cells were counted using trypan blue dye exclusion with 0.4% trypan blue solution.

B. Cell viability/ trypan-blue exclusion assay

A simple method of measuring cell viability in cell culture is to count viable cells using the trypan blue dye exclusion method. The technique is based on the disruption of the cell membrane that distinguishes non-viable from viable cells. The disrupted membranes of nonviable cells allow the trypan blue dye to be absorbed up by the cell, and thus viable cells can be visualized under the microscope as white cells

compared to the blue-colored non-viable cells. H1792 and MDA-F471 cells were seeded in triplicate in 96-well plates at a density of 3,000 cells/100 μ l and 2,000 cells/100 μ l per well respectively, in complete media (with 10% FBS). Cells were incubated overnight in the incubator then treated in triplicates with two concentrations of various sulfated alginates in 100 μ l complete media for 24 and 48 hrs. After 24 hrs of treating the cells, we disregarded the supernatants containing the dead cells, while the live cells were harvested by adding 50 μ l trypsin/ EDTA. We neutralized the trypsin by adding 100 μ l of media, then 50 μ l of cell suspension was mixed with 50 μ l of trypan blue. Live cells were counted on the four corner chambers of a hemocytometer by using the previously mentioned formula. The same procedure was repeated after 48hrs. Similarly, the same procedure was done on RWPE1 cells, but in 1 % collagen-coated 24-well plates (as described before) at a density of 20,000 cells/ ml. Data were reported as mean \pm SEM.

C. Cell growth assay/MTT

The anti-proliferative effect of H1792 and MDA-F471 was measured *in vitro* by using the MTT (3-(4, 5- dimethylthiazol-2-yl)-2, 5-diphenyltetrazolium bromide) assay. Cells were plated in 100 μ l complete medium in 96-well culture plates at the densities like ones used in trypan blue assay. Cells were incubated overnight in the incubator then treated in triplicates with two concentrations of various sulfated alginates in 100 μ l complete media for 24 and 48 hrs. For each time point, 10 μ l of 5 mg/ml (in 1x PBS) MTT reagent was added to each well and incubated at 37°C for 4 hours. As the result, metabolically active/viable cells could convert the yellow tetrazolium salt (MTT)

into insoluble purple formazan crystals due to the high levels of NADH and NADPH, which is a measure of mitochondrial metabolic activity. Then, we added 100µl of stop dye solution into each well to dissolve the formazan crystals and stop the reaction. Finally, after overnight incubation, the reduced MTT optical density (OD) was measured at a wavelength of 595 nm using an ELISA reader (Multiskan Ex). The percentage of cell viability was expressed as percentage growth relative to control wells and treated wells at different concentrations. Data were reported as mean \pm SEM.

D. Wound healing/scratch assay

A wound-healing assay is used to study the directional migration of the cells *in vitro*. It is an important assay that mimics the cellular migration *in vivo* and allows the study of cellular interactions between cells and their ECM to control the migration of the cells (Gebäck et al., 2009). We seeded H1792 and MDA-F471 cells on a 12-well plate using a concentration of 100 µg/ml of the various sulfated alginates and incubated them until they reached 80 % to 90 % confluence. After that, 2 µg/ml of mitomycin C (with an original concentration of 0.5 mg/ml that was dissolved in PBS) was added into each well between 15-25 mins. Then, we discarded the media and scraped the monolayer of cells in the middle using a 200 µl micropipette tip. After that, the plates will be washed twice with PBS to remove the detached cells. Remaining cells were cultured in complete media with or without treatment. Microscopic photos were subsequently taken at 0, 6, 18, 24, and 48 hrs. The distance traveled by the cells into the wounded area was computed from the closure of the wounds and expressed as a percentage of the wound closure upon treatment compared to the control condition. The

images were taken using Leica software and we measured the distance of the wound using Zen software, in which the data represented mean \pm SEM of three independent experiments.

E. Sphere formation assay

1. Seeding

Cells were washed with 1X PBS, followed by adding trypsin, then centrifuged at 900rpm for 5 minutes and the pellet was resuspended in cold serum-free DMEM/ F-12 medium. Cells were counted using a hemocytometer and trypan blue dye for the exclusion of dead cells by the previously mentioned formula. Afterward, 2,000 cells/well were suspended in growth factor-reduced MatrigelTM (Corning)/serum-free medium (1:1) in a total volume of 50 μ l/well on a 24-well plate. Cells were seeded uniformly in a circular manner around the bottom rim of each well and allowed to solidify in the incubator at 37°C for 45 minutes. Then, 500 μ l of warm medium (5 % FBS) was added gently in the middle of each well and incubated in a humidified incubator (5% CO₂) at 37°C. Spheres were replenished with a new fresh medium every three days. After seven days, spheres were counted and the sphere-forming unit (SFU) was calculated as follows: $SFU = 100 \times (\text{number of xiovert inverted light microscope was formed spheres}/2,000)$. Bright-field images of formed spheres were taken using the Zeiss Aed. Adherent cells grown will be referred to as parental cells and sphere-forming cells will be noted as CSC.

2. Propagation of spheres

After we counted and took pictures for the formed spheres, we propagated them, in which aspirated the media from the center of each well and replaced it with 500 μ l of 0.5 mg/ml dispase (Gibco) solution dissolved in the growth medium. Then, we incubated them for 45 minutes in a humidified incubator at 37°C. Dispase breaks down the Matrigel™ and releases the spheres into the medium. The released spheres were then collected and centrifuged at 1200 rpm for 7 mins. The pellet was resuspended in 0.05 % Trypsin-EDTA and incubated for 12 mins (MDA-F471) or 6 mins (H1792) at 37°C, to dissociate the spheres into single cells. Trypsin was then neutralized by the addition of an equal volume of growth medium containing 5 % FBS, followed by centrifugation at 900 rpm for 5 minutes. Cells were resuspended in serum-free medium, counted and re-plated as explained before. However, on the first day of propagation of second generation of spheres (G2), we added our treatment at concentration of 100 μ l/ml of media, in which 500 μ l of media and treatment was added gently in the middle of each well in triplicates for control, pure alginates and DS 2.7, while duplicates per other conditions. The vehicle control contained 10 % serum-free media which is equivalent to the amount present in the maximum concentration of μ L of alginates. Spheres were replenished every three days with fresh media and drugs. After seven days, we repeated the same procedure done on the spheres of G1 and we evaluated the SFU, using the previously mentioned formula, and the area of the spheres formed ($\text{Area}=\pi(d/2)^2$), but we stopped at the step of dispase, in which we discarded the supernatant, and we washed them with 1XPBS, we centrifuged at 1200 rpm for 5 mins and we snap-freeze

the spheres in liquid nitrogen. They were stored on -80C, to be used in RNA extraction. The experiments were repeated three times and the data was reported as mean \pm SEM.

F. Total RNA extraction

Total RNA was extracted from frozen pellets of MDA-F471 and H1792 dissociated spheres which had been snap-frozen in liquid nitrogen and stored at -80°C. According to the manufacturer's protocol, the RNeasy Plus Mini Kit (Qiagen) was used for the extraction procedure. First, 350 μ l of buffer RLT Plus containing 10 μ l/1 ml β -mercaptoethanol (β -ME), a highly denaturing guanidine isothiocyanate containing buffer which immediately denatures RNases by reducing the disulfide bonds to ensure isolation of intact RNA, was added to the cell pellet and homogenized at 4°C by pipetting up and down with a 22-gauge syringe needle and vortexing to ensure complete cell lysis and membrane disruption. Then, the cell lysate was centrifuged for 3mins at maximum speed. The supernatant was mixed with an equal volume of freshly prepared 70 % ethanol with RNase-free water to provide appropriate RNA-binding conditions, then transferred to 2 ml RNeasy spin column and pulse centrifuged for 15 secs. The RNeasy spin column with the membrane-bound RNA was washed with 700 μ l Buffer RW1 and pulse centrifuged for 15secs. After that, the RNeasy spin column was washed two more times with 500 μ l Buffer RPE and centrifuged for 2mins at 14,000 rpm, to discard contaminants. Finally, the RNeasy spin column was placed in a new 1.5 ml collection tube and 26 μ l of RNase-free water was carefully added directly to the spin column membrane and left standing for 5mins to allow the membrane to soak. The tube was then centrifuged for 1min at 14,800 rpm to elute the RNA, then transferred and

stored at -80°C. To evaluate the purity and concentration of eluted RNA, the samples were placed on ice and the absorbances of 2 µl of each sample or RNase-free water (used as blank) were measured using DeNovix DS-11FX Spectrophotometer. The 260/280 ratio was used to assess the purity of RNA and a ratio of ~2.0 was considered as pure RNA.

G. Two-Step Quantitative Real-Time Polymerase Chain Reaction (qRT-PCR)

We continued the quantification of genes by qRT-PCR, focusing mainly on their mode of expression, down-regulated or up-regulated in the spheres. We analyzed the genes of humans (Table1) and murine (Table2).

1. Reverse transcription of RNA to cDNA

Total RNA samples were reverse transcribed into cDNA using the QuantiTact Reverse Transcription Kit (Qiagen) following the manufacturer's protocol. Total RNA samples and reagents of the kit were placed on ice at room temperature for 10 //mins. Then, we dissolved the tubes by vortexing, followed by briefly centrifuging to collect residual liquid from the sides of the tubes, and then kept them on ice to minimize the risk of RNA degradation. Genomic DNA (gDNA) was eliminated by adding 2 µl to 0.5 µg of RNA sample and free-RNase water in a total elimination reaction volume of 14 µl. Then, we incubated the tubes for 2 mins/ at 42°C. We followed the elimination reaction with reverse-transcription reaction, in which we prepared the master mixes to be used in this reaction, containing all the following components per one reaction:

Reverse-transcription master mix 1 µl

Quantiscript RT buffer	4 μ l
RT Primer Mix	1 μ l

Then, 6 μ l of master mixes were added to each tube and mixed gently. The tubes were incubated for 15 mins at 42°C, followed by incubation for 3 mins at 95°C. Finally, we diluted the cDNA with free-RNase water to reach 40 μ l and stored the reverse-transcription reactions at -20°C.

2. *Quantitative real-time PCR (qRT-PCR)*

All qRT-PCR experiments were carried under sterile conditions using filtered tips and molecular grade free-RNase water in technical duplicates for one time, in which two more runs are under progress. The primer oligonucleotide sequences (Table 1 & 2) were found in published studies. Primer mixture was prepared by combining 10 μ l of reverse and forward primers each with 80 μ l free-RNase water and stored at -20°C. A master mix for each transcript reaction was prepared as follows:

Free-RNase water	2.5 μ l
2X buffer	5 μ l
Primer mixture	0.5 μ l

After distributing 2 μ l of cDNA to each well, we added 8 μ l of the prepared master mix to each well of a skirted 384 qRT-PCR(Bio-Rad). A no-template control well was prepared in each transcript reaction with 2 μ l of free-RNase water instead of cDNA. Once the plate was prepared, we sealed it using an adhesive sealer, centrifuged briefly and loaded into a BioRad CFX 384 qRT-PCR machine. The qRT-PCR thermal cycling conditions which included a melt curve specific for the product are summarized

in Table 3. We analyzed the obtained data using the $2^{-\Delta\Delta Ct}$ calculation method by normalizing to two conserved reference genes: Glyceraldehyde 3-phosphate dehydrogenase (*GAPDH*) and TATA-box binding protein (*TBP*), in which these two genes were suggested in the expression analysis of CSCs' genes (Lemma et al., 2016). Gene expression is computed and analyzed with respect to the control. The PCR experiments were performed three times with duplicates or both cell lines, but the extraction of RNA from spheres is one of the challenging experiments. This led to taking only one experiment of the PCR out of three independent experiments, and we will do the other experiments, just after my thesis defense.

Human gene	Primer Sequence (5'-3')	Annealing Temp.(°C)	Reference
<i>ALDH1A1</i>	F-TGTTAGCTGATGCCGACTTG	60	(E. Kim et al., 2008)
	R-ATTCTTAGCCCGCTCAACACT		
<i>ALDH3A1</i>	F- GCAGACCTGCACAAGAATGA	60	(Levi et al., 2009)
	R-TGTAGAGCTCGTCCTGCTGA		
<i>CCL20</i>	F-GGTGAAATATATTGTGCGTCTCC	60	(Luan et al., 2017)
	R-ACTAAACCCCTCCATGATGTGC		
<i>GAPDH</i>	F-GGACCTGACCTGCCGTCTA	60	(Msheik et al., 2020)
	R- TGGTGCTCAGTGTAGCCCAG		

Table 1: Primer sequences and annealing temperature of some selected human genes.

Murine gene	Primer Sequence (5'-3')	Annealing Temp.(°C)	Reference
<i>Alcam</i>	F-ATGGCATCTAAGGTGTCCCCT	60	(E. Kim et al., 2008)
	R-AGACGGCAAGGCATGACAA		
<i>Aldh1a1</i>	F-GACAGGCTTTCCAGATTGGCTC	60	(Levi et al., 2009)
	R-AAGACTTTCCACCATTGAGTGC		
<i>Ccl20</i>	F-GTGGGTTTCACAAGACAGATG	57	(Sato et al., 2017)
	R-TTTTCACCCAGTTCTGCTTTG		

<i>Gapdh</i>	F-GCAAAGTGGAGATTGTTGCCA	60	(Patin et al., 2018)
	R-GCCTTGACTGTGCCGTTGA		
<i>Tbp</i>	F-CCTTGTACCCTTCACCAATGAC	60	(Gong et al., 2016)
	R-ACAGCCAAGATTCACGGTAGA		
<i>Tnf</i>	F-TCAGCCGATTTGCTATCTCATA	57	(Sha et al., 2014)
	R-AGTACTTGGGCAGATTGACCTC		

Table 2: Primer sequences and annealing temperature of some selected murine genes.

Step	Polymerase Activation	Amplification (40cycle)			Melt Curve
		Denaturation	Annealing	Extension	
Temperature (°C)	95	95	Variable	72	65-95 in 0.5 increments
Time	5min	15sec	30sec	30sec	5sec/step

Table 3: Thermal cycling conditions of qRT-PCR.

H. Statistical analysis

Statistical analysis was done using GraphPad Prism 7 software. One-way ANOVA test was performed to determine whether there are any significant differences among the means of three or more independent groups, followed by Bonferroni corrected multiple comparison test to compare the differences between each test group and the control. Statistical significance was reported when the p-value was less than 0.05. (*p<0.05; **p<0.01; ***p<0.001)

CHAPTER III

RESULTS

A. The effect of different DS of SulfAlg *in vitro* on the viability of LUAD cells using Trypan Blue exclusion assay

To begin with, we wanted to assess the effect of the increase in the DS of sulfated alginates at two different concentrations (10 µg/ml and 100 µg/ml) on the viability of H1792 and MDA-F471 cells using trypan blue exclusion assay. It was shown that the viability of H1792 cells was not significantly decreased with the increase in the DS of alginates (Figure 7A & 7B). Similarly, MDA-F471 cells stated an insignificant decrease in the viability of the cells at the concentration of 10 µg/ml of different DS of alginates (Figure 7C). However, at concentration of 100 µg/ml, MDA-F471 showed significant decrease in the cell viability of MDA-F471 with the increase in the DS of sulfated alginates to DS 2.0, DS 2.7 and heparin, in which DS 2.7 showed significant decrease by about 50% in cell viability with $p < 0.001$ after 24 and 48hrs of treatment (Figure 7D).

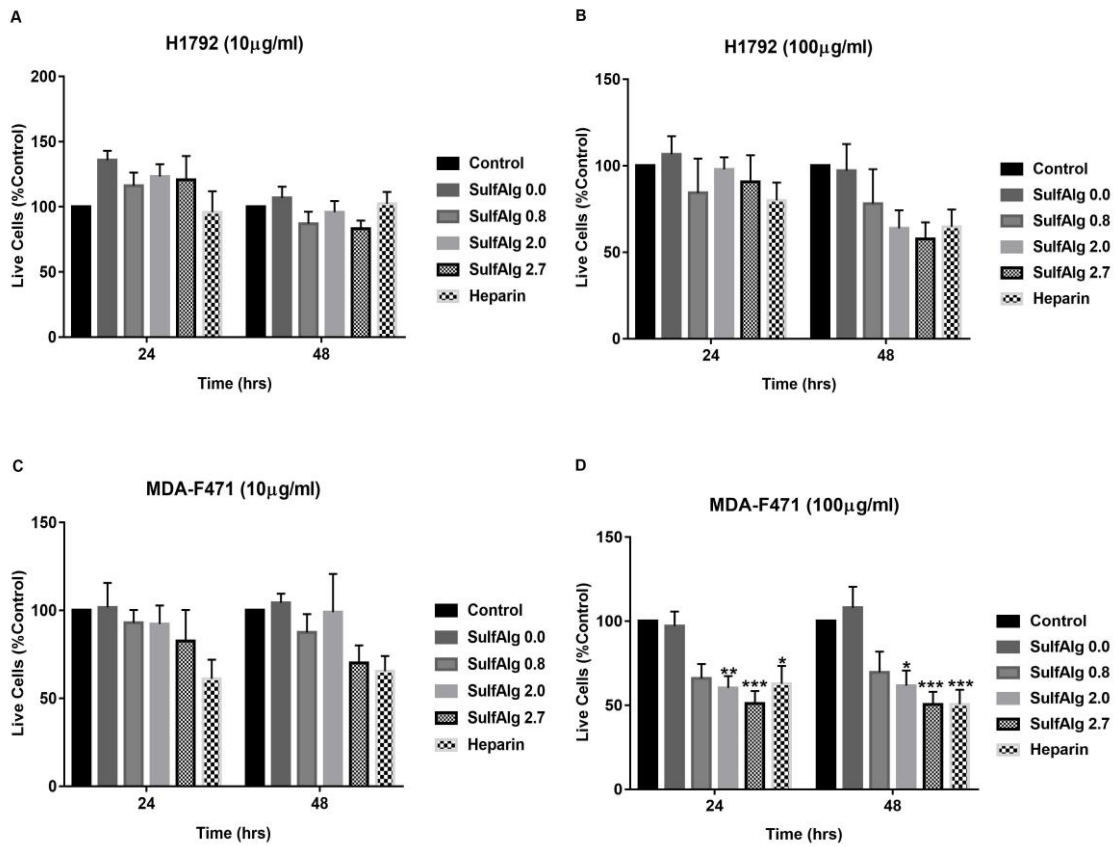
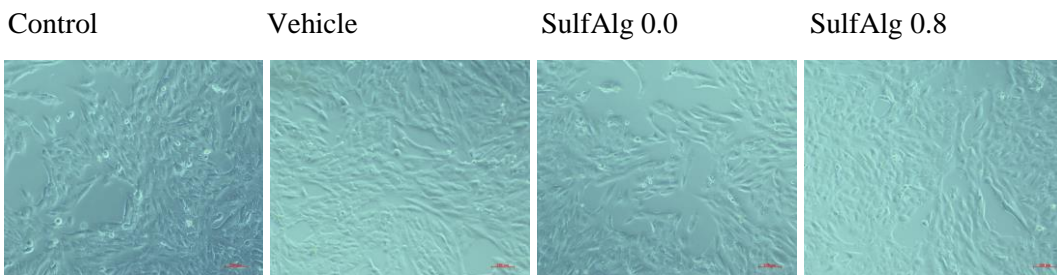
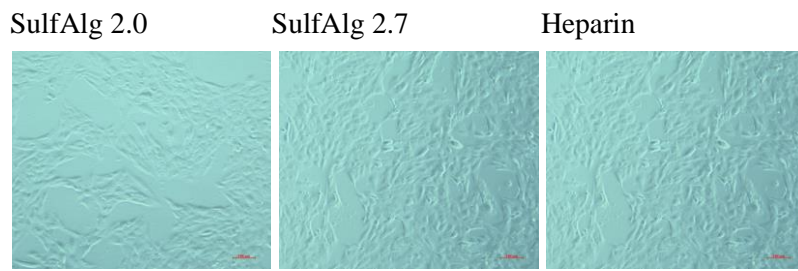


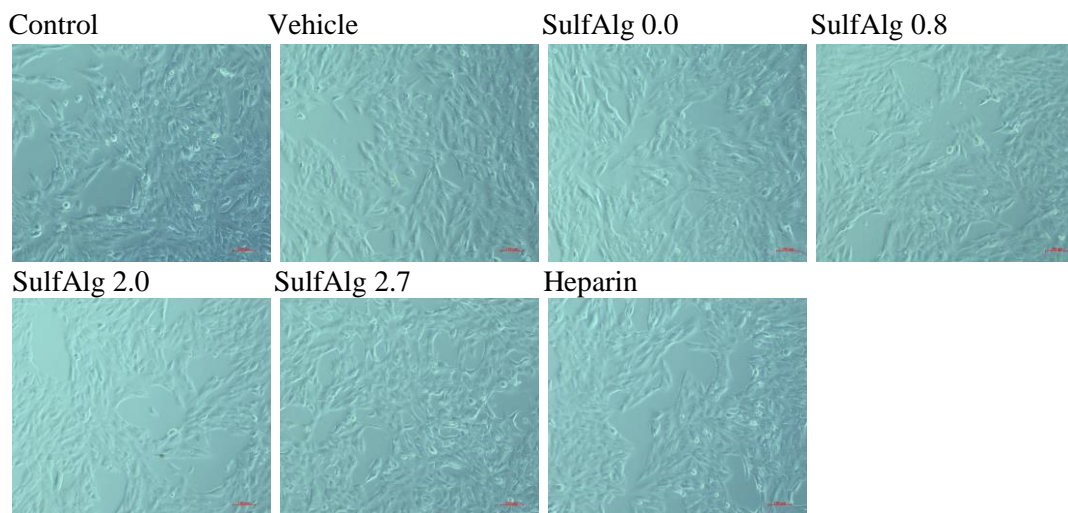
Figure 7: The effect of different DS of alginates on the number of live H1792 and MDA-F471 at the two concentrations (10µg/ml & 100µg/ml). H1792 and MDA-F471 were treated with different DS of alginates at two concentrations and two-time points. Cells were counted in triplicates measurement using the trypan blue exclusion method and results are represented as the percentage with respect to control (complete media). Data represent an average of six independent experiments (mean ± SEM) (*p<0.05, **p<0.01, ***p<0.001).

A

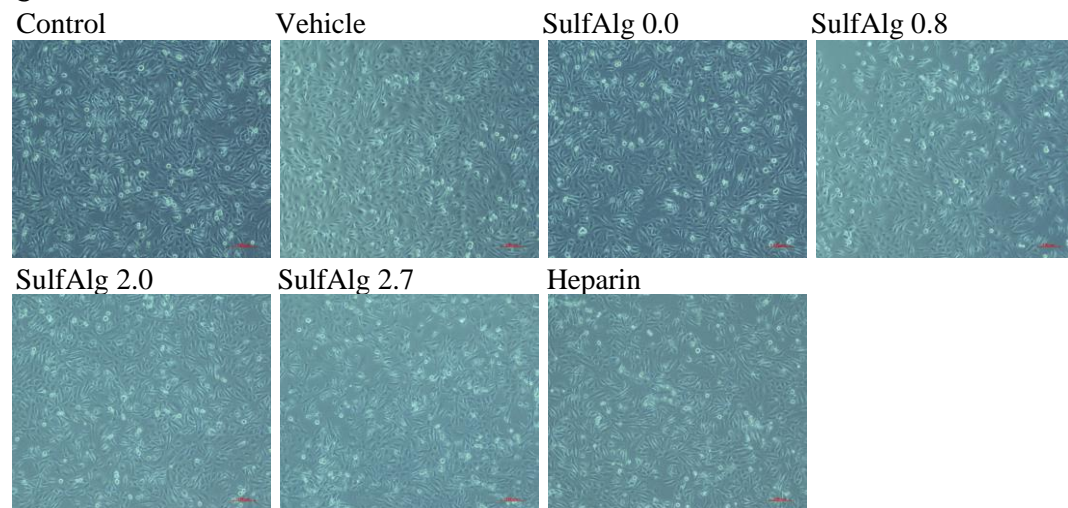




B



C



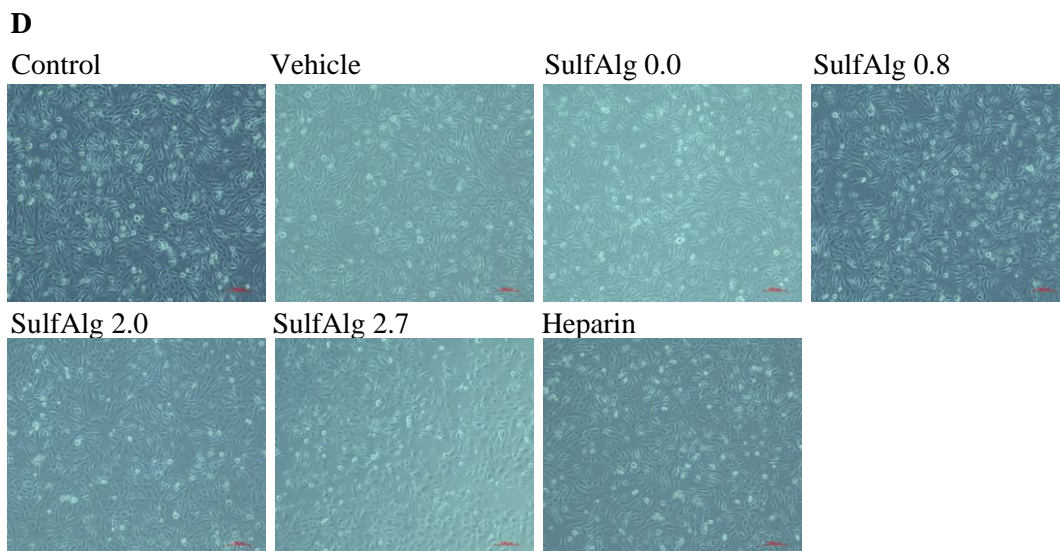


Figure 8: The effect of the increase in the DS of mimetic GAGs on the morphology of H1792 and MDA-F471 cells. H1792 and MDA-F471 cells were treated with different DS of alginates with concentrations of 10 $\mu\text{g/ml}$ (A and C) and 100 $\mu\text{g/ml}$ (B and D) for 24hrs, respectively. Representative images were taken using an Axiovert inverted microscope and analyzed by Carl Zeiss Zen 2012 image software. Scale bar = 100 μm .

To verify that the high decrease of sulfation does not affect normal epithelial cells, we performed trypan blue assay on prostatic human RWPE1 cells. it was found that the increase of sulfation increases the cell viability, but this increase was insignificant (Figure 9).

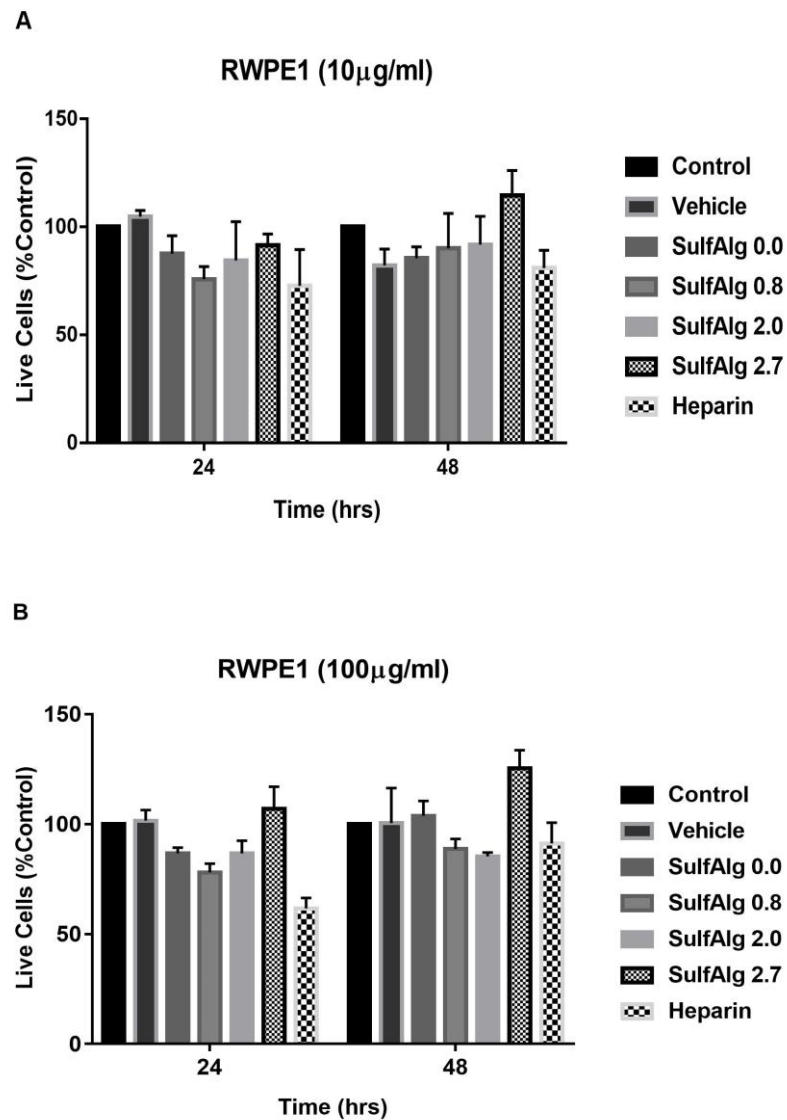


Figure 9: The effect of different DS of alginates on the cell viability of RWPE1 at the two concentrations (10µg/ml & 100µg/ml). Data were recorded as mean ± SEM.

B. Effect of increase in DS of alginates at two concentrations on the proliferation of human and murine LUAD cells using MTT assay *in vitro*

The research aimed to assess the effect of the increase in the DS of mimetic GAGs on the proliferation of H1792 and MDA-F471 cells using MTT assay. As a result, the proliferative activity of H1792 cells was not significantly altered with the

increase in the DS of sulfated alginates at the two different concentrations (Figure 10A and 10B). Similarly, the proliferation of MDA-F471 cells was insignificant with the increase in the DS of alginates, but there was a trend that showed a decrease in their proliferative activity with the increase in the alginate's DS. Thus, the increase of the DS of alginates did not affect the growth of LUAD human and murine cells.

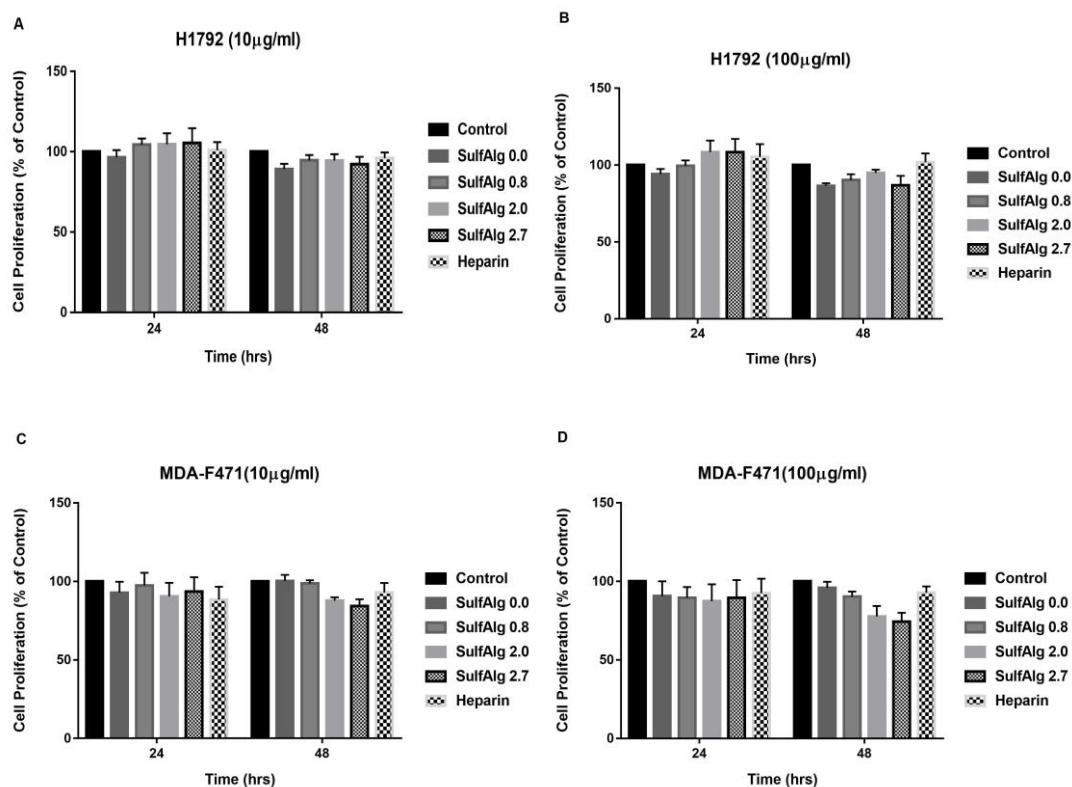


Figure 10: The effect of different DS of sulfated alginates at the two concentrations (10 µg/ml and 100 µg/ml) on H1792 and MDA-F471 cells' proliferation using MTT assay. The proliferation of H1792 (A&B) and MDA-F471 (C&D) is relatively resistant to various DS of alginates at the two concentrations (10 µg/ml & 100 µg/ml). Results are expressed as a percentage of a treated group compared to its control. Data represent an average of 6 independent experiments and are expressed as mean ± SEM.

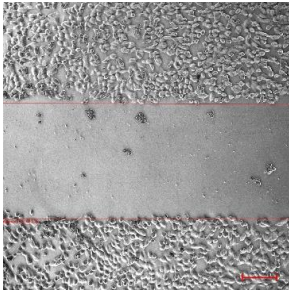
C. The increase in the DS of alginates inhibits the migration of H1792 and MDA-F471 *in vitro*

Metastasis is necessary for the growth and mortality of lung cancer cells. To investigate the role of variation in DS on LUAD cell migration, wound healing/scratch assay was performed. The results showed that the wound is completely closed in control and DS 0.0 of MDA-F471 after 24hrs and of H1792 after 48hrs. However, the migration of tumor cells was suppressed after 6hrs after treatment with DS 2.0, DS 2.7 and heparin, in both cell lines.

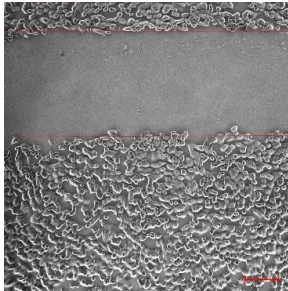
Remarkably, the increase in the DS of alginates reduced the rate of wound closure of LUAD cells in treated wells compared to control and DS 0.0. Although the formed wound was completely healed in control and DS 0.0 after 24hrs and 48hr, of MDA-F471 and H1792 respectively, the alginate of DS 2.0 significantly suppressed the migration of the treated cells to close the wound by about 50% in H1792 and 65% in MDA-F471, after 48hrs and 24hrs respectively ($p < 0.001$). Similarly, the alginate of DS 2.7 significantly reduced the migration of the treated cells by about 50% in H1792 (Figure 13A) and 68% in MDA-F471 (Figure 13B) ($p < 0.001$). Also, these results were revealed by the microscopic images of the scratches in the 12-well plate, using 200 μ l tip, Figure 11 and Figure 12, respectively for H1792 and MDA-F471. Thus, the increase in the DS of alginates suppresses the migration of the LUAD cells like heparin.

T0

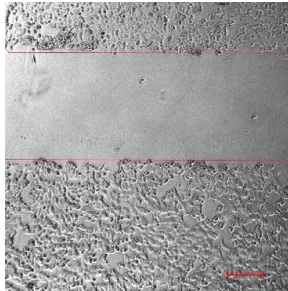
Control



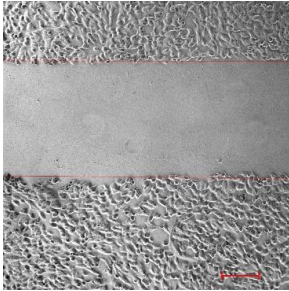
SulfAlg 0.0



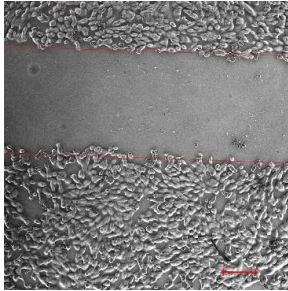
SulfAlg 0.8



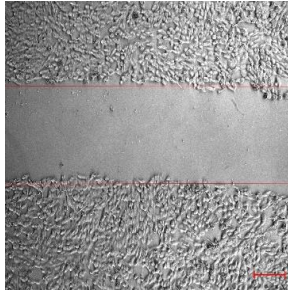
SulfAlg 2.0



SulfAlg 2.7

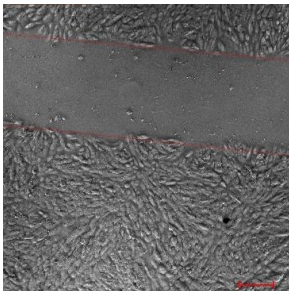


Heparin

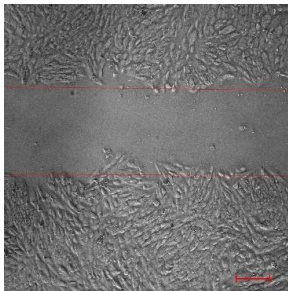


T6

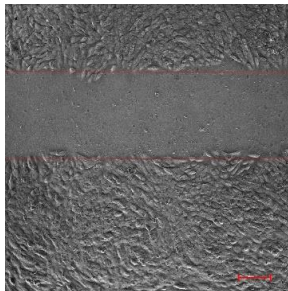
Control



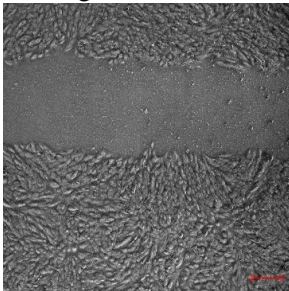
SulfAlg 0.0



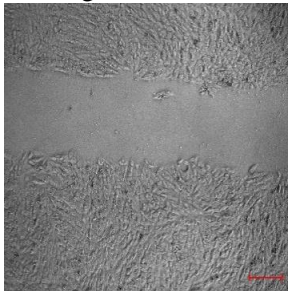
SulfAlg 0.8



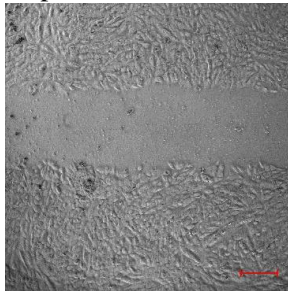
SulfAlg 2.0



SulfAlg 2.7



Heparin

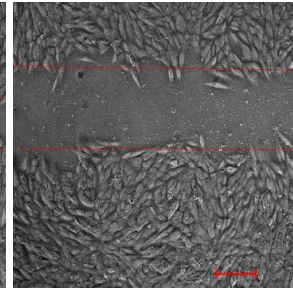
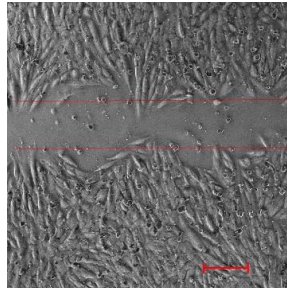
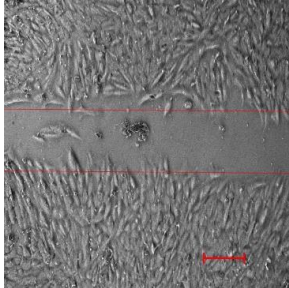


T18

Control

SulfAlg 0.0

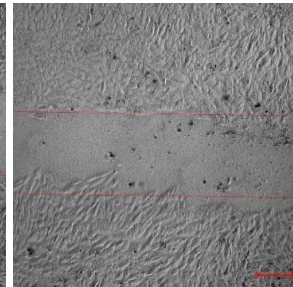
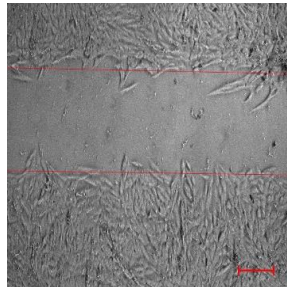
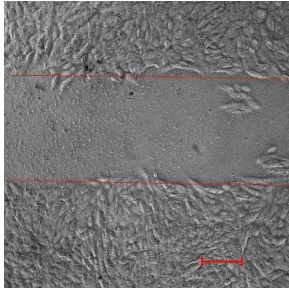
SulfAlg 0.8



SulfAlg 2.0

SulfAlg 2.7

Heparin

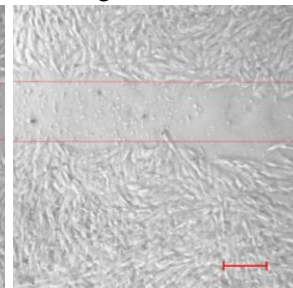
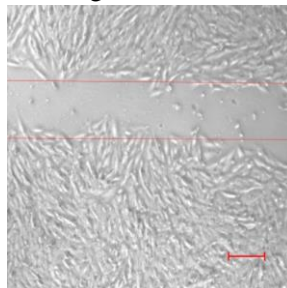
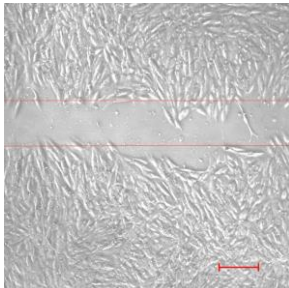


T24

Control

SulfAlg 0.0

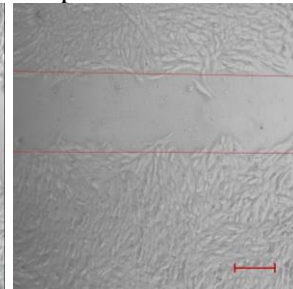
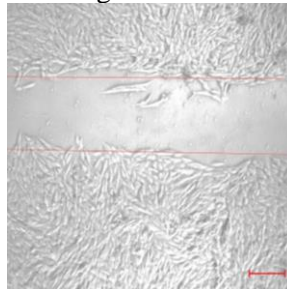
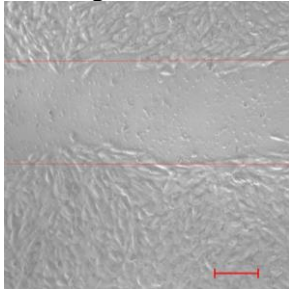
SulfAlg 0.8



SulfAlg 2.0

SulfAlg 2.7

Heparin



T48:

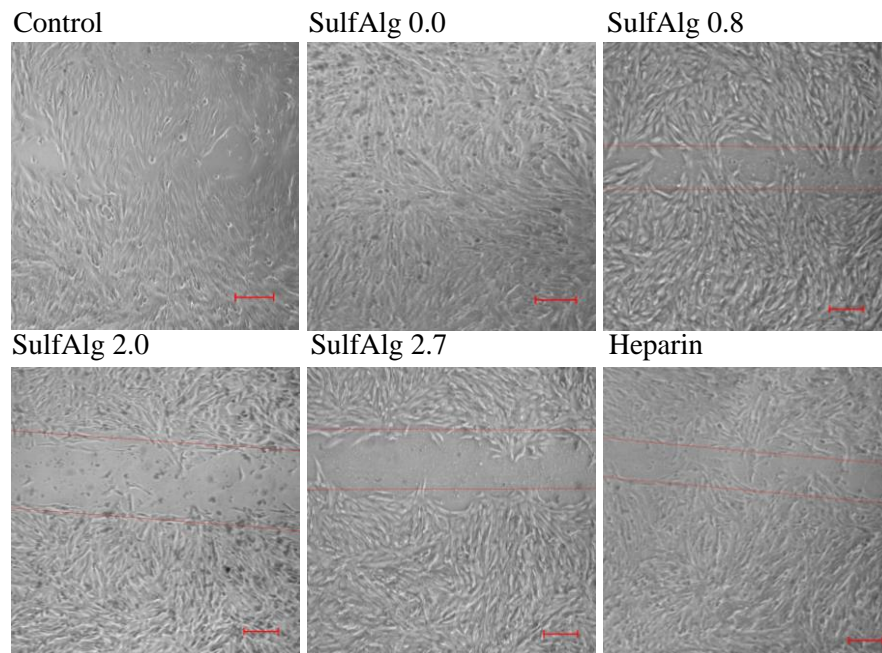
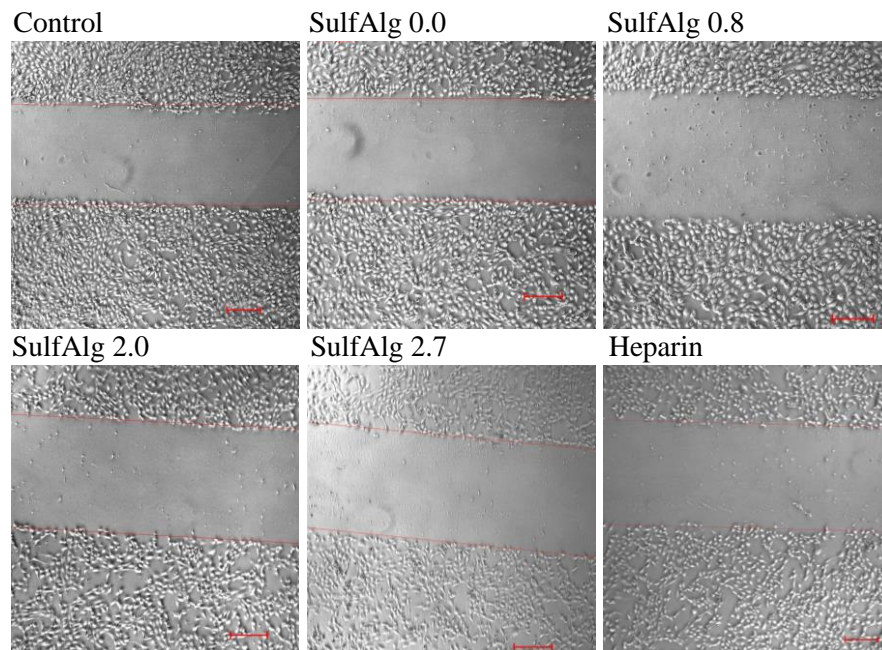


Figure 11: Representative images of H1792 cells showing the effect of the increase in sulfation of alginates on cell migration. A scratch was made in a 12-well plate of confluent H1792 cells with Mitomycin C, using a 200 μ l tip, and images were taken at T=0, 6, 18, 24, and 48 hrs with or without treatment, and quantification of closure distance was determined over time. Scale bar= 100 μ m.

T0:

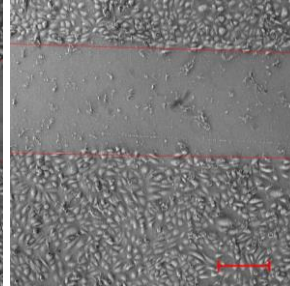
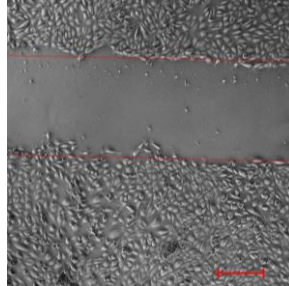
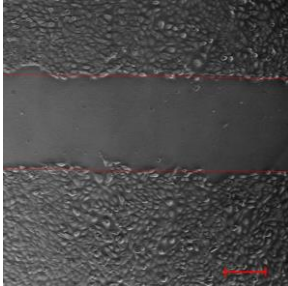


T6:

Control

SulfAlg 0.0

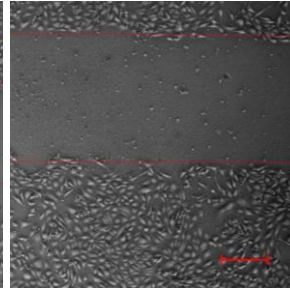
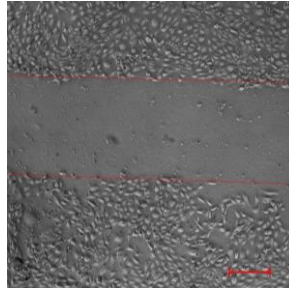
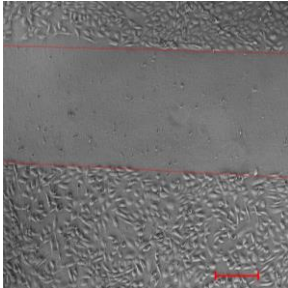
SulfAlg 0.8



SulfAlg 2.0

SulfAlg 2.7

Heparin

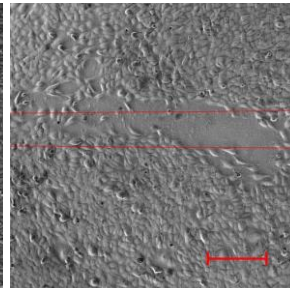
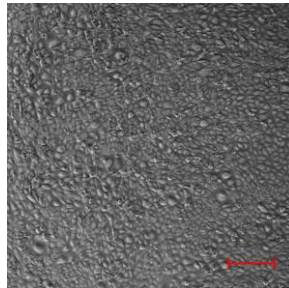
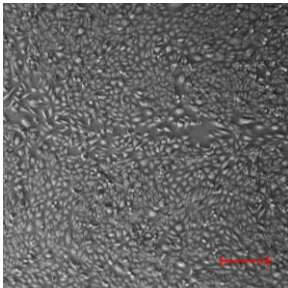


T18:

Control

SulfAlg 0.0

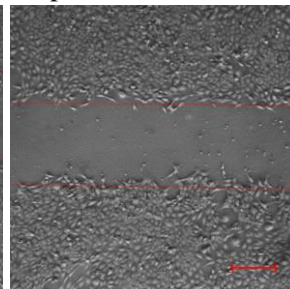
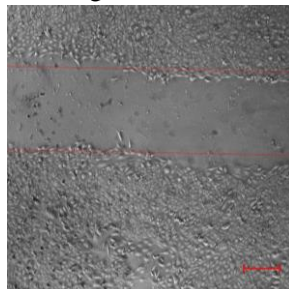
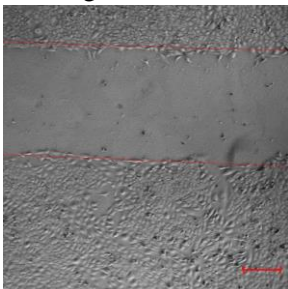
SulfAlg 0.8



SulfAlg 2.0

SulfAlg 2.7

Heparin

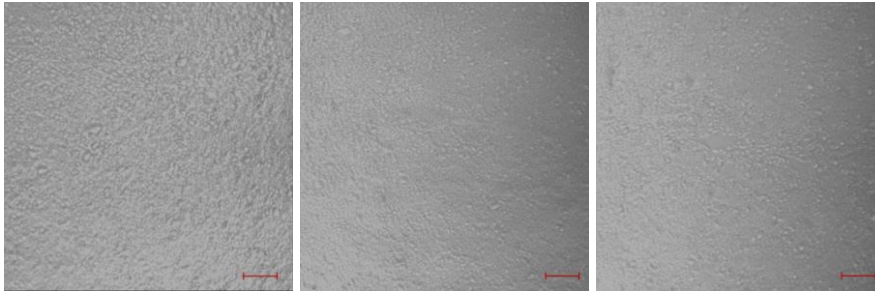


T24:

Control

SulfAlg 0.0

SulfAlg 0.8



SulfAlg 2.0

SulfAlg 2.7

Heparin

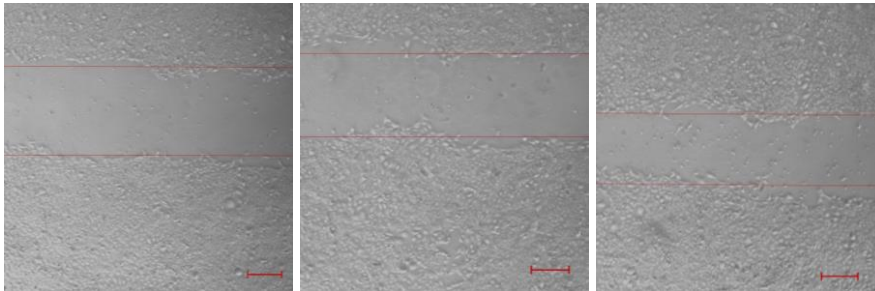


Figure 12: Representative images of MDA-F471 showing the effect of the increase of DS of alginates on cell migration. A scratch was made in a 12-well plate of confluent MDA-F471 cells with Mitomycin C, using a 200 μ l tip, and images were taken at T=0, 6, 18, and 24hrs with or without treatment, and quantification of closure distance was determined over time. Scale bar= 100 μ m.

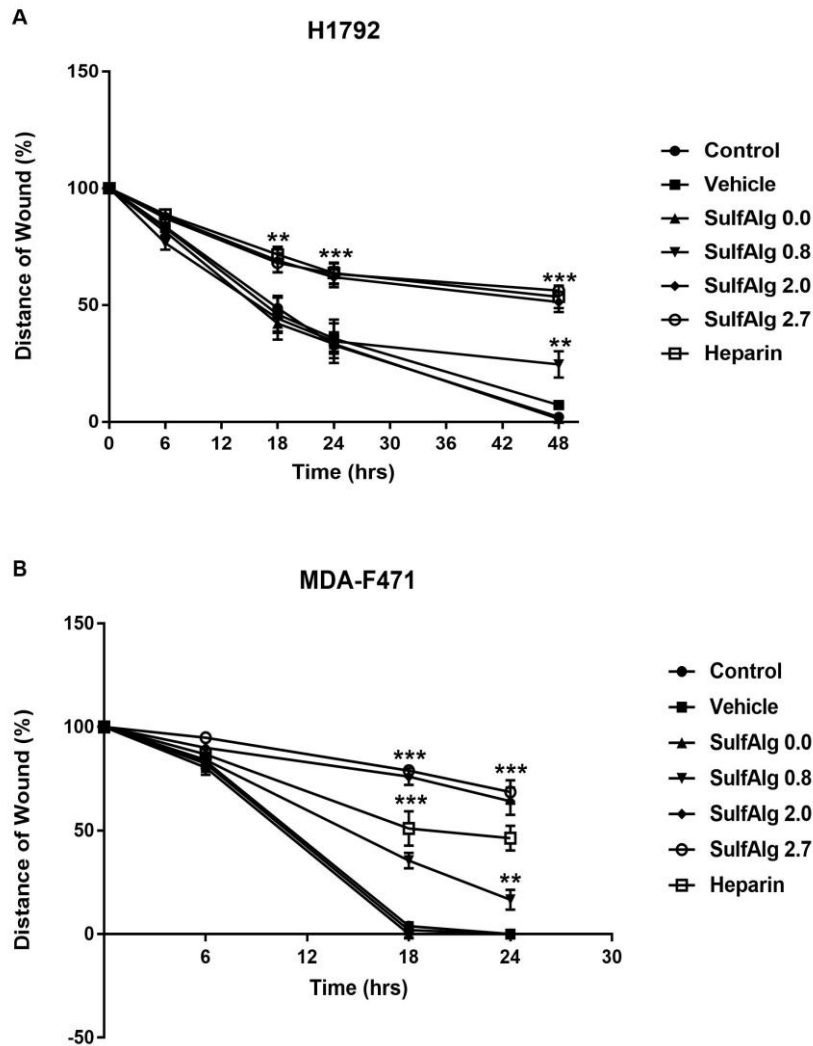


Figure 13: The increase in the sulfation of GAGs reduces the migratory potentials of human and murine KRAS-mutant LUAD cells. Results indicate that the increase in the sulfation of GAGs mimicked by the increase in the DS of alginates (DS=0.8, 2.0, 2.7) significantly inhibits the migratory abilities of H1792 (A) and MDA-F471 (B) at different time points (6, 18, 24, and 48hrs), while the wound on untreated cells and treated cells with alginates of DS=0.0 monolayer completely closed after 48hrs for H1792 and 24hrs for MDA-F471. Alginates with DS=2.0 and DS=2.7 and heparin halted the migration of H1792 cells by almost 45% and MDA-F471 by almost 30%, 48hrs, and 24hrs post-treatment respectively. Data are represented as mean \pm SEM (* p <0.05, ** p <0.01, *** p <0.001).

D. The increase in the DS of alginates reduces the sphere formation capacity in murine and human LUAD cells

1. Effect of increase in DS on the sphere formation unit (SFU)

One of the important aims in our study is to show the effect of the increase in DS of sulfated alginates, in which the high DS 2.0 and 2.7 mimic heparin, on cancer CSCs of LUAD. Thus, this aim is fulfilled using the sphere formation assay (3D culture). A single-cell suspension of H1791 and MDA-F471 were cultured in Matrigel™ for 7 days to enrich the CSCs of LUAD, then the formed spheres were propagated to G2 and treated by different DS of alginates with the concentration of 100µm/ml for another 7 days. The formed spheres were counted using an inverted light microscope and images were taken on the same day using ZEN software (Figure 14). Later, the number and size of the formed spheres were analyzed and reported as SFU and average area of spheres. The results showed that the number and size of spheres decreased significantly with the increase of the DS of alginates.

It was reported that the SFU of H1792 (Figure 14A) and MDA-F471 (Figure 14B) decreased significantly in the DS 0.8, DS 2.0, DS 2.7 and heparin with $p < 0.001$. The control and DS 0.0 alginates treated wells of both H1792 and MDA-F471 showed almost SFU=9. Compared to the control, the DS 0.8 reported a significant decrease in the SFU by almost 30% ($p < 0.001$) in both cell lines. However, the DS 2 and DS 2.7, similar to heparin, stated a significant decrease in SFU by almost 60% in the two cell lines ($p < 0.001$). Thus, the SFU decreased as the increase in the DS of alginates.

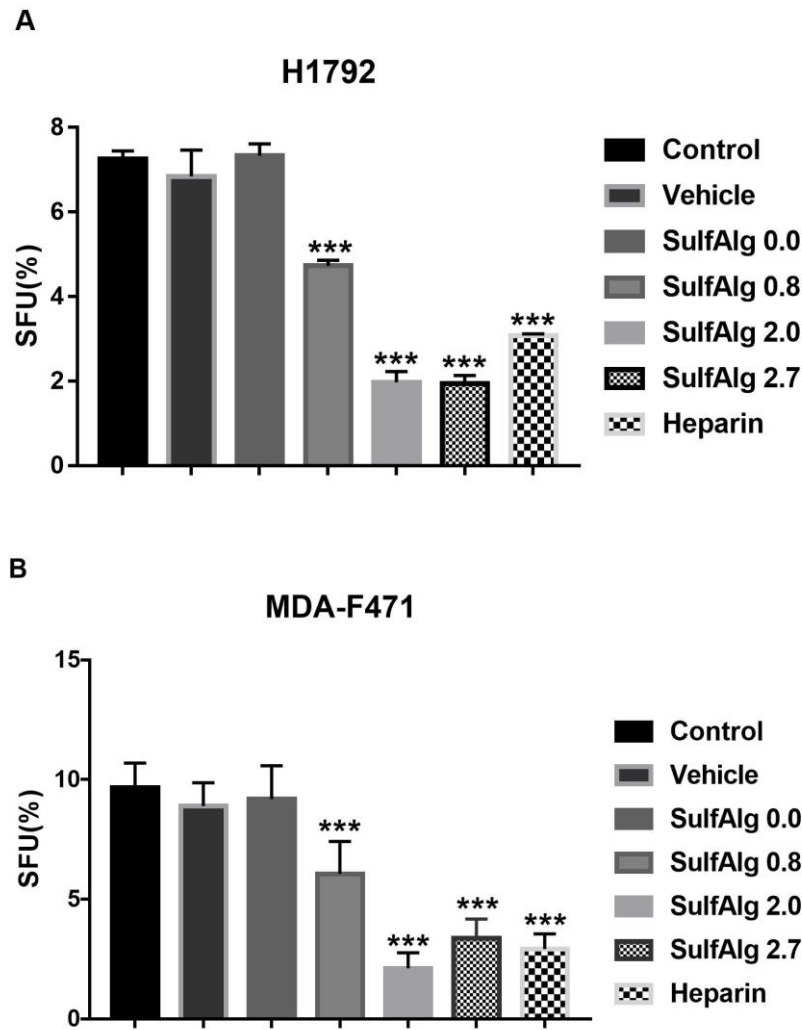


Figure 14: Effect of increase in DS of alginates on SFU of H1792 and MDA-F471. Spheres formed in each well, represented as G2, were counted after 7 days. Results showed that the increase in DS of alginates to DS 2.0 and DS 2.7 significantly reduced the SFU of both cell lines. DS 2.0 and DS 2.7 reduced the SFU of both H1792 cells (A) and MDA-F471 by almost 60% (B). Data are reported as mean \pm SEM (* p <0.05, ** p <0.01, *** p <0.001).

2. Effect of increase in DS on the area of a formed sphere (μm^2)

Similarly, the increase in the DS of alginates reduced the ability of the CSC population of H1792 and MDA-F471 to form spheres with large diameters. The area of the spheres formed decreased with the increase in the DS of alginates. The DS 0.0 alginates-treated wells reported similar results to the control. With the increase in the

DS of alginates to DS 0.8, the area of the spheres decreased significantly by 40%, compared to the control ($p < 0.001$). With a further increase in DS of alginates to DS 2.0 and DS 2.7, the area of the formed sphere of H1792 (Figure 15A) and MDA-F471 (Figure 15B) decreased significantly by about 50% and 60%, respectively, like heparin ($p < 0.001$). Also, these results were revealed by the microscopic images taken for the spheres formed at G2, Figure 16 and Figure 17 for H1792 and MDA-F471 respectively.

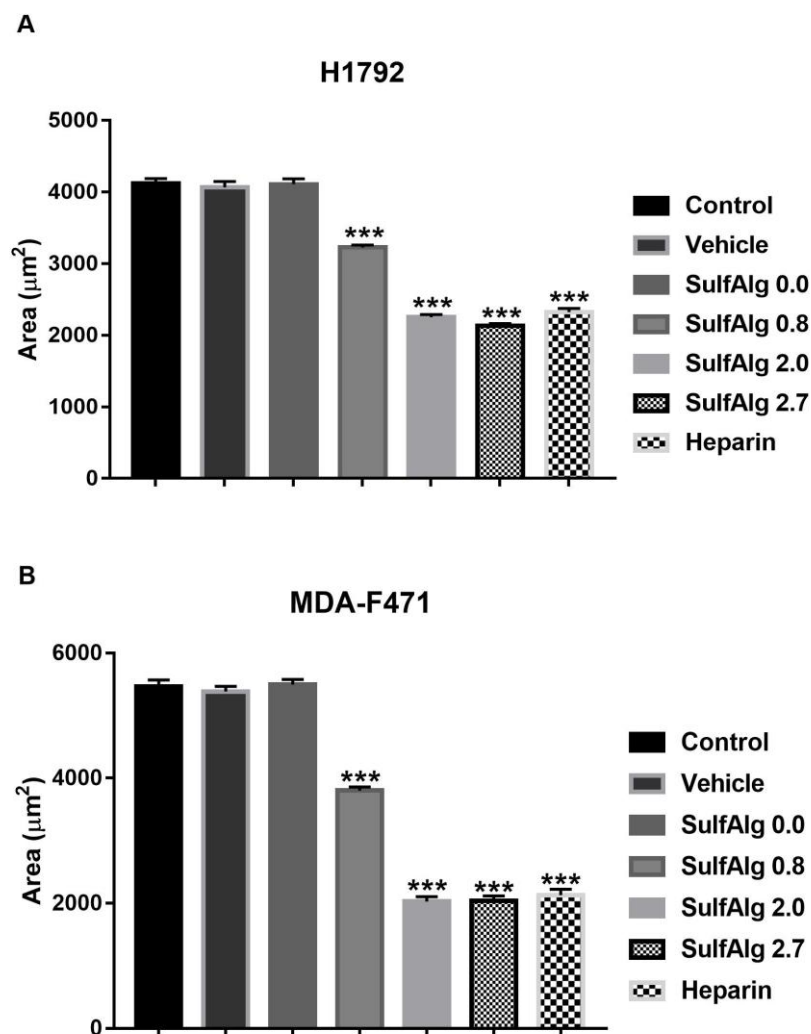


Figure 15: The effect of the increase in DS of alginates on the area of the spheres formed of both human and murine LUAD cells. The effect of the increase in DS of alginates on the area of the spheres formed of both human and murine LUAD cells. Spheres formed in each well, represented as G2, were counted after 7 days. Results showed that the increase in DS of

alginates to DS 2.0 and DS 2.7 significantly reduced the area of both cell lines. DS 2.0 and DS 2.7 reduced the SFU of H1792 cells (A) and MDA-F471(B) by almost 50% and 60%, respectively. Data are represented as mean \pm SEM (* p <0.05, ** p <0.01, *** p <0.001).

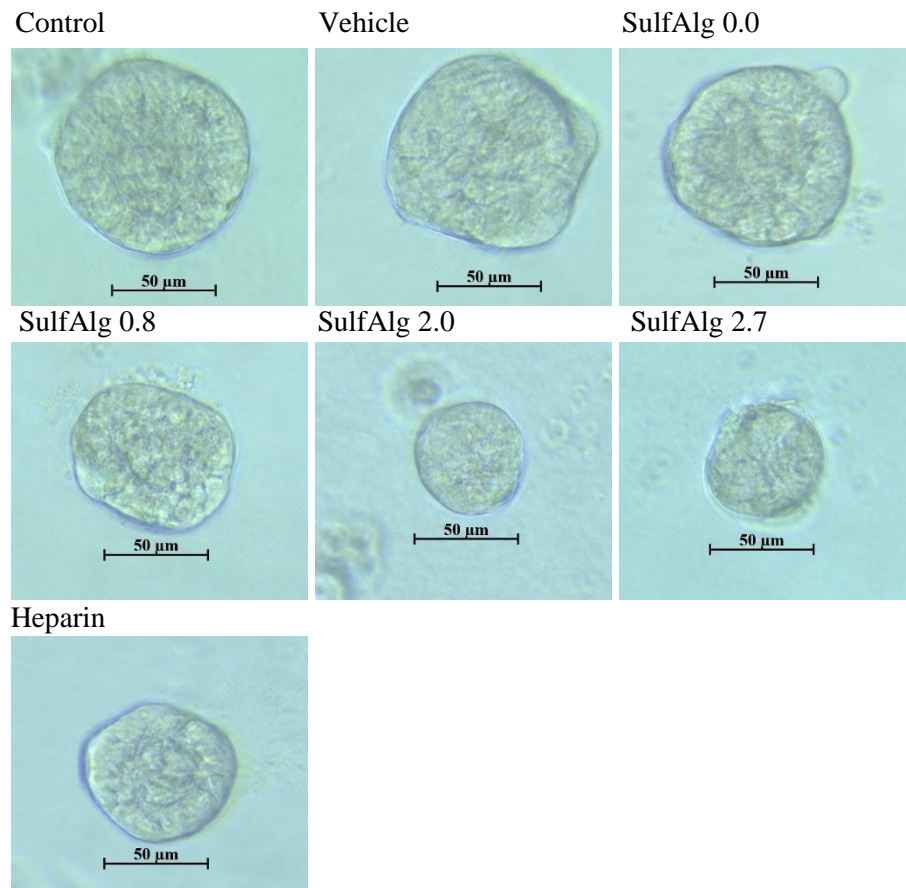


Figure 16: Diameters of H1792 spheres after treatment G2 spheres with different DS of alginates. Representative bright-field images of H1792 G2 spheres with the increase in the DS of alginates. Images were visualized by Axiovert inverted microscope and analyzed by Carl Zeiss Zen 2012 image software. Scale bar = 50 μ m.

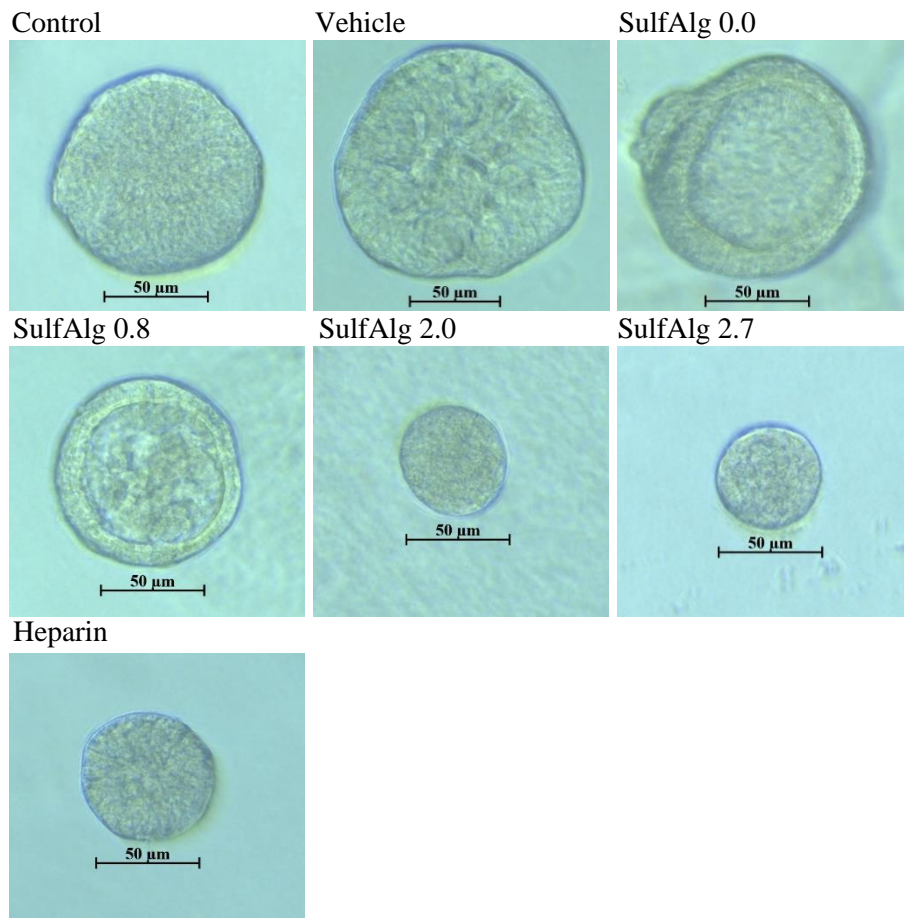


Figure 17: Diameters of MDA-F471 spheres after treatment G2 spheres with different DS of alginates. Representative bright-field images MDA-F471 G2 spheres with the increase in the DS of alginates. Images were visualized by Axiovert inverted microscope and analyzed by Carl Zeiss Zen 2012 image software. Scale bar = 50µm.

E. The expression of some genes in human *KRAS*- mutant and murine *K-Ras* – mutant LUAD spheres

As mentioned in the methodology chapter, we determined the effect of the increase of sulfation on the mode of differential expression, upregulation or downregulation, of human and murine spheres of G2 through the process of qRT-PCR.

1. Effects of increase in the DS of alginates on the expression of some genes in human KRAS-mutant LUAD cells

After the collection of human spheres of G2, we used them to test for the expression of genes of CSCs. It was proven that *ALDH1A1* and *ALDH3A1* are important in the maintenance and self-renewal of CSCs of various tumors, while *CCl20* promotes chemokines (Huang et al., 2009). Thus, we wanted to assess the effects of the increase in DS of alginate on the expression of CSCs markers. We determined that the increase in the DS of alginates downregulated the expression of *ALDH1A1*, *ALDH3A1*, and *CCL20*. Although these experiments will be repeated 2 more times to do statistical analysis, we can conclude that the increase in DS of alginates leads to the downregulation of the surface markers of stemness of human LUAD CSCs.

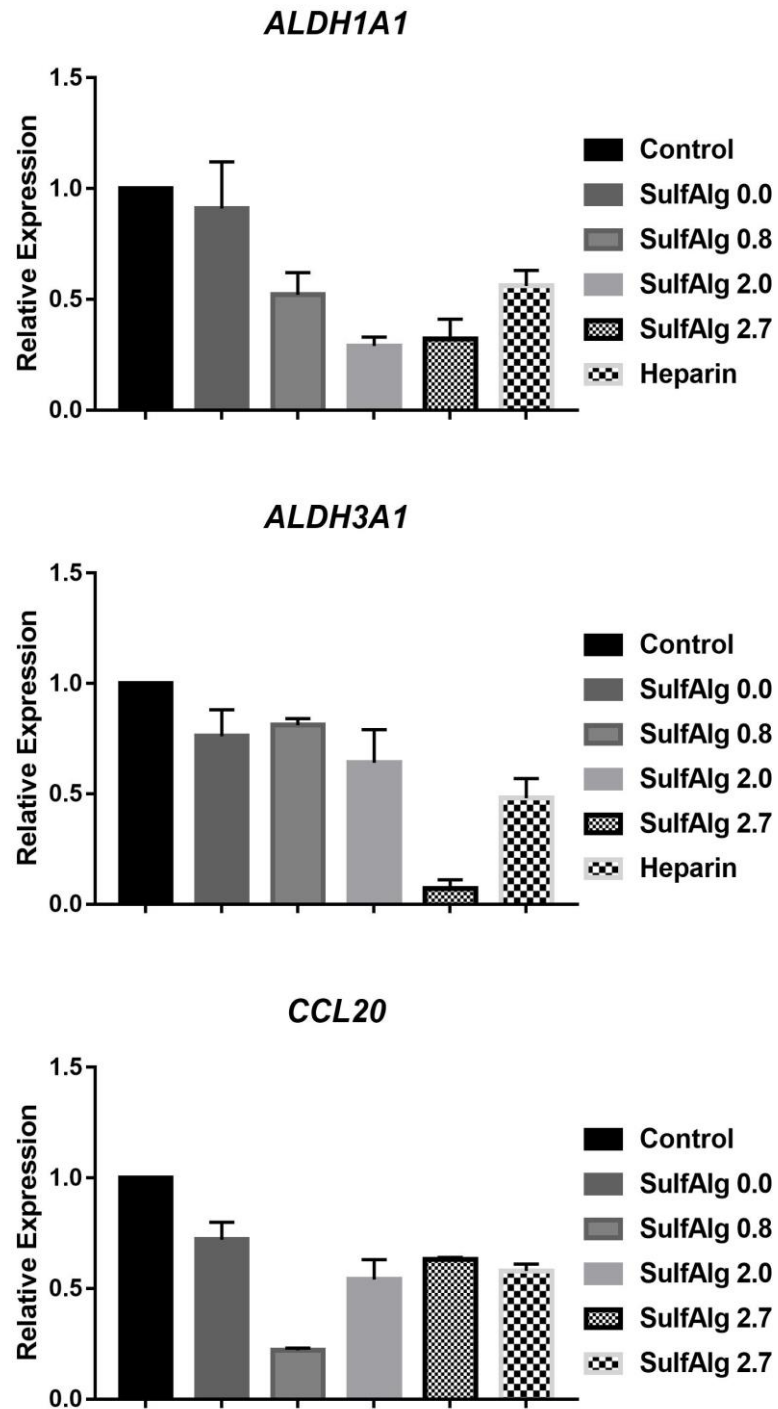
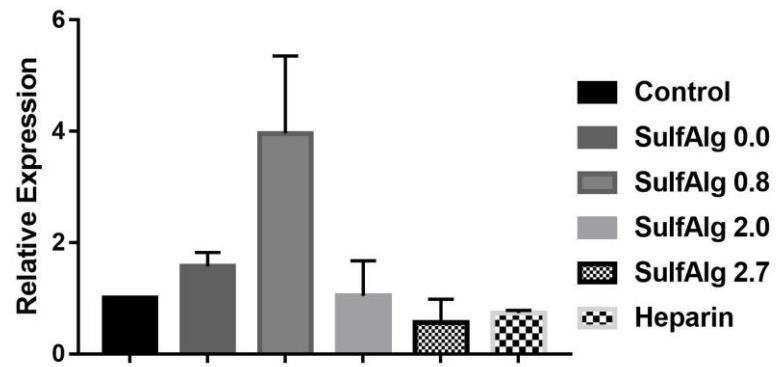


Figure 18: Differential expression of selected stemness markers in H1792 spheres by qRT-PCR. Downregulation of *ALDH1A1*, *ALDH3A1*, and *CCL20* in G2 spheres was determined by qRT-PCR and analyzed using the $2^{-\Delta\Delta C_t}$ calculation by normalization to two different conserved reference genes (*GAPDH*) and is represented as mean \pm SEM (n=1).

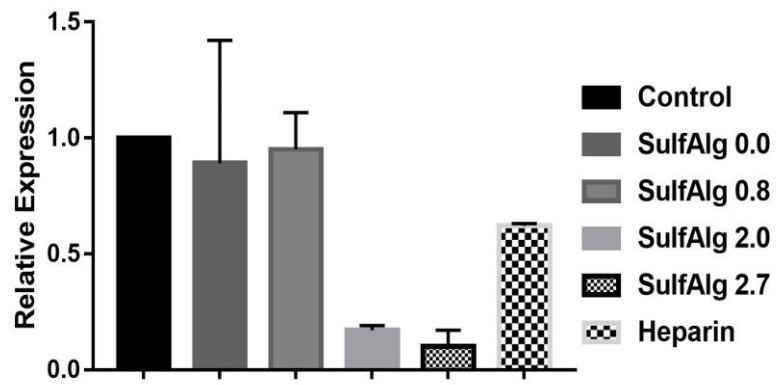
2. Effects of increase in the DS of alginates on the expression of some genes in murine KRAS-mutant LUAD cells

After the collection of murine spheres of G2, we used them to test for the expression of genes of CSCs. It was proven that *Aldh1a1* is important for the maintenance and self-renewal of CSCs of various tumors, *Alcam* is a well-known surface marker for lung epithelial CSCs, and *Ccl20* and *Tnf* promote chemokines. Thus, we wanted to assess the effects of sulfation on the expression of CSCs markers. We determined that the increase in the DS of alginates downregulated the expression of *Alcam*, *Aldh1a1*, *Ccl20*, and *Tnf*. Although these experiments will be repeated 2 more times to do statistical analysis, we can reveal that the increase in the DS of alginates downregulates the expression of murine LUAD CSCs' surface markers.

Alcam



Aldh1a1



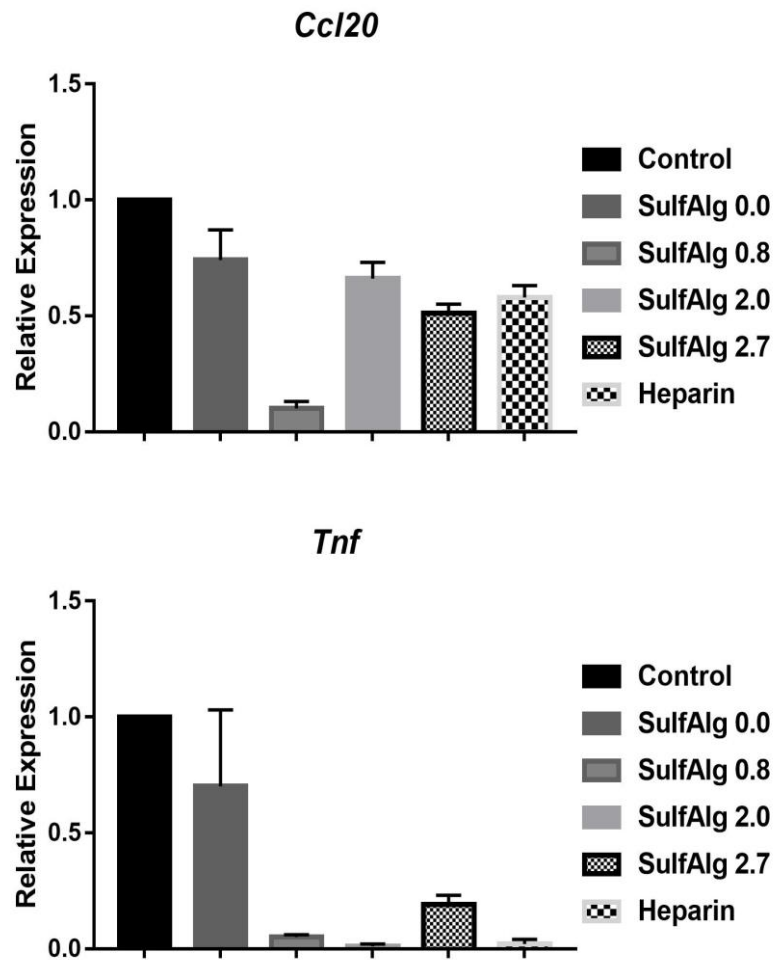


Figure 19: Differential expression of selected stemness markers in MDA-F471 spheres by qRT-PCR. Downregulation of *Alcam*, *Aldh1a1*, *Ccl20*, and *Tnf* in G2 spheres was determined by qRT-PCR and analyzed using the $2^{-\Delta\Delta C_t}$ calculation by normalization to two different conserved reference genes (*Gapdh* and *Tbp*) and is represented as mean \pm SEM (n=1)

CHAPTER IV

DISCUSSION

Lung adenocarcinoma with a mutation in the *KRAS* oncogene is the most aggressive and prevalent alveolar subtype of lung cancer with resistance to most therapies (Zappa & Mousa, 2016). Since tumors are due to the cellular mutations leading to dysfunctionality in the ECM and its components such as GAGs, determining the role of sulfated GAGs in suppressing the proliferative and cellular abilities of the cancerous cells is very important in target therapy. Several studies have shown the diverse roles of sulfated GAGs, especially heparin, in many cellular activities. Heparin, which is the most sulfated GAGs, is very effective in anticoagulation, angiogenesis, and binding to GFs (Capila & Linhardt, 2002; Hoppensteadt et al., 2012; Sasisekharan & Venkataraman, 2000). Moreover, heparin regulates tumor growth by forming a fibrin barrier around the tumor. Thus, leads to the formation of new blood vessels and stimulates the immune system to fight the tumor (Hoppensteadt et al., 2012). Many studies showed the effect of heparin on tumor suppression, including pancreatic cancer, metastatic breast cancer, and LUAD cancer (Hejna et al., 1999; Zhang et al., 2016), in which the downregulation of heparin was observed in cancerous cells, while heparin's re-expression enhanced apoptosis of carcinoma cells (Lai et al., 2003). Heparin has effective roles not only on the cancerous cells but also on CSCs, in which heparin enhances the ABCG2 protein degradation, thus decreasing the CSCs' chemo-resistant through affecting signaling pathways (Niu et al., 2012). However, the isolation of

heparin molecules with equal DSs is very complicated. As a result, scientists mimic heparin and other sulfated GAGs by different sulfation methods in which the hydroxyl groups in the alginate backbone are replaced using sulfating agents, such as SO_3^- complexes and HClSO_3 acid formamide. Sulfated alginates mimic heparin by binding to plenty of GFs involved in cellular activities (Øystein Arlov & Skjåk-Bræk, 2017). In this thesis, sulfated alginates have been used with different DSs as biomimetic molecules of sulfated GAGs (DS 0.0, DS 0.8, DS 2.0 and DS 2.7), in addition to heparin from intestinal porcine.

Moreover, sulfated polysaccharides were proven to have anti-tumor properties in which they suppressed the cell proliferation of hepatoma cultured in 2D (M. Yu et al., 2017). Sulfated polysaccharides from edible seaweed, *Undaria pinnatifida*, have anti-proliferative and migratory effects on the tumor (Xiaolin Xu et al., 2019). On the other hand, sulfated polysaccharides extracted from brown algae enhanced the proliferation and growth of normal chondrocytes and their markers' expression by maintaining the binding of GFs (Mhanna et al., 2013). Also, several studies have shown the importance of CSCs in initiating tumor growth (Pine et al., 2008; Z. Yu et al., 2012). The normal stem cells express special surface markers, in which their overexpression allows the isolation of CSCs, but these findings are not so accurate. Eramo and his coworkers isolated lung CSCs that overexpressed an extensive proliferation and self-renewal marker called CD133. The isolation of CSCs is still challenging so scientists proved that sphere formation assay enriches the cells with stem-like properties from primary tumors and cell lines (Hardavella et al., 2016; Pine et al., 2008). This assay enables the

researchers to determine the effects of the drugs on the proliferation and genes' expression of CSCs-like. Therefore, we hypothesized the effects of the increase in the sulfation of mimetic GAGs by different DS of alginates will reduce the proliferation, migration and CSC-like properties of human and murine LUAD cells. Knowing that these sulfated alginates mimic sulfated GAGs by binding to GFs.

First, we assessed the anti-tumor properties of biomimetic sulfated GAGs on the two *K-Ras* mutant LUAD cell lines, the murine *Gprc5a*^{-/-} (p.G12D) LUAD cells and the human H1792 LUAD line (with a codon 12 KRAS variant), by investigating the effects of the increase of DS of alginates (DS=0.0, 0.8, 2.0 and 2.7) at two different concentrations 10 µg/ml and 100 µg/ml, dissolved in media with 0% FBS on the proliferation, number of live cells and migration of LUAD cells *in vitro*. Results showed that the increase in the DS of biomimetic sulfated GAG had no effect on the proliferation and viability of H1792 cells in a dose and time-dependent manner, by MTT assay and trypan blue assay respectively. Similarly, the proliferation of MDA-F471 cells was not affected by the increase in the sulfation of alginates at low doses of 10 µg/ml. On the other hand, the viability of MDA-F471 cells decreased significantly with the increase in the sulfation of alginates with respect to the control at concentration 100 µg/ml, but not at concentration 10 µg/ml. These results indicated that the increase in the sulfation of GAGs mimicking by different DSs of alginates did not affect the proliferation of the tumor. Thus, sulfated GAGs do not have anti-proliferative properties against human and murine LUAD cells, yet they have an effect on the total number of murine LUAD cells. However, other studies showed that sulfated polysaccharides

reduce the proliferation of carcinoma (Xiaolin Xu et al., 2019; M. Yu et al., 2017). Also, we determined the effect of biomimetic molecules on the proliferation of normal epithelial cells and the results showed that with the increase in the sulfation of mimetic sulfated GAGs, the cells proliferated the most at DS=2.7. These results agreed with the study of Mhanna and his coworkers which showed that sulfated alginate enhances the proliferation of normal chondrocytes and the expression of chondrocyte markers (Mhanna et al., 2014). Furthermore, the ability of the cancerous cells to metastasize to other organs is the lethal level of cancer. Thus, we assessed, through 2D wound healing/migration assay, the effects of the increase in sulfation of GAGs on the migratory abilities of the two cell lines at concentration 100 µg/ml. A significant decrease was observed in the ability of metastatic murine and human *K-Ras* mutant LUAD cells to migrate. This suggests that the increase in the sulfation of GAGs, mimicking by different DSs of alginates, has high inhibitory effects on metastasis, thus on tumorigenicity of LUAD cells. Thus, these results are consistent with previous results which showed that sulfated polysaccharides had anti-migratory properties against tumor (Xiaolin Xu et al., 2019; M. Yu et al., 2017). However, it remains to be assessed whether the increase of DS of alginates inhibits the proliferation and metastasis of LUAD animal models and the underlying molecular mechanisms of the actions of these biomimetic molecules.

Then, we aimed to determine the ability of the increase in sulfation of alginates on target SP of CSCs of H1792 and MDA-F471 using the 3D culture system with MatrigelTM *in vitro* (Daouk et al., 2019). We used the 3D model using MatrigelTM since

it is closer to the *in vivo* environment and provides more reliable results by mimicking ECM (Daley et al., 2008). Based on the previous study for our team, we isolated the LUAD CSCs formed using sphere formation assay at G2 since they found that the expression of surface markers of stem-like cells was significantly expressed at G2 and G5 (Daouk et al., 2019). As a result, we assessed the effects of different DSs on the CSCs-like of H1792 and MDA-F471. Results showed that the increase in the sulfation of biomimetic GAGs decreased significantly the SFU as well as the size of the spheres of both human and murine LUAD cells. Therefore, we conclude that the sulfated GAGs and their analogous using different DSs of alginates are effective in targeting the CSC population of *KRAS* mutant LUAD. These results are consistent with previous studies that showed the effects of antitumor drugs on targeting subpopulation of CSC of *KRAS*-mutant driven LUAD using sphere formation assay (Daouk et al., 2019; Hardavella et al., 2016). However, it is the first time to assess the effects of sulfated alginates on SP of CSCs using sphere formation assay.

To conclude, this is the first study to show the effects of sulfated GAGs and different DSs of alginates on the anti-tumorigenic properties of cancerous and CSCs population in *KRAS*-mutant LUAD. However, the mechanism by which sulfated GAGs act on the LUAD is still not understood so further experiments can be done to see if these biomimetic molecules bind to GFs instead of natural polysaccharides in the LUAD cells or if they enhance the anti-tumor properties by acting on signaling pathways or they have their own mechanism of action. Also, this study shed the light on the effective usage of sulfated alginates as a potential treatment for *KRAS*-mutant

LUAD and pave the way for future studies, such as applying sulfated alginates on animal models with KRAS-mutant LUAD and see their effects *in vivo*.

BIBLIOGRAPHY

- Afratis, N., Gialeli, C., Nikitovic, D., Tsegenidis, T., Karousou, E., Theocharis, A. D., Pavão, M. S., Tzanakakis, G. N., & Karamanos, N. K. (2012). Glycosaminoglycans: Key players in cancer cell biology and treatment. *The FEBS Journal*, 279(7), 1177–1197. <https://doi.org/10.1111/j.1742-4658.2012.08529.x>
- Arlov, Ø, Öztürk, E., Steinwachs, M., Skjåk-Bræk, G., & Zenobi-Wong, M. (2017). Biomimetic sulphated alginate hydrogels suppress IL-1 β -induced inflammatory responses in human chondrocytes. *European Cells & Materials*, 33, 76–89. <https://doi.org/10.22203/eCM.v033a06>
- Arlov, Øystein, Aachmann, F. L., Feyzi, E., Sundan, A., & Skjåk-Bræk, G. (2015). The Impact of Chain Length and Flexibility in the Interaction between Sulfated Alginates and HGF and FGF-2. *Biomacromolecules*, 16(11), 3417–3424. <https://doi.org/10.1021/acs.biomac.5b01125>
- Arlov, Øystein, & Skjåk-Bræk, G. (2017). Sulfated Alginates as Heparin Analogues: A Review of Chemical and Functional Properties. *Molecules*. <https://doi.org/10.3390/molecules22050778>
- Arlov, Øystein, & Skjåk-Bræk, G. (2017). Sulfated Alginates as Heparin Analogues: A Review of Chemical and Functional Properties. *Molecules : A Journal of Synthetic Chemistry and Natural Product Chemistry*, 22(5). <https://doi.org/10.3390/molecules22050778>

- Arlov, Øystein, Skjåk-Bræk, G., & Rokstad, A. M. (2016). Sulfated alginate microspheres associate with factor H and dampen the inflammatory cytokine response. *Acta Biomaterialia*, *42*, 180–188.
<https://doi.org/10.1016/j.actbio.2016.06.015>
- Barrowcliffe, T. W. (2012). History of Heparin. In R. Lever, B. Mulloy, & C. P. Page (Eds.), *Heparin—A Century of Progress* (Vol. 207, pp. 3–22). Springer Berlin Heidelberg. https://doi.org/10.1007/978-3-642-23056-1_1
- Birchmeier, C., Birchmeier, W., Gherardi, E., & Vande Woude, G. F. (2003). Met, metastasis, motility and more. *Nature Reviews. Molecular Cell Biology; London*, *4*(12), 915–925. <http://dx.doi.org.ezproxy.aub.edu.lb/10.1038/nrm1261>
- Boolell, V., Alamgeer, M., Watkins, D. N., & Ganju, V. (2015a). The Evolution of Therapies in Non-Small Cell Lung Cancer. *Cancers*, *7*(3), 1815–1846.
<https://doi.org/10.3390/cancers7030864>
- Boolell, V., Alamgeer, M., Watkins, D. N., & Ganju, V. (2015b). The Evolution of Therapies in Non-Small Cell Lung Cancer. *Cancers*, *7*(3), 1815–1846.
<https://doi.org/10.3390/cancers7030864>
- Capila, I., & Linhardt, R. J. (2002). Heparin–Protein Interactions. *Angewandte Chemie International Edition*, *41*(3), 390–412. [https://doi.org/10.1002/1521-3773\(20020201\)41:3<390::AID-ANIE390>3.0.CO;2-B](https://doi.org/10.1002/1521-3773(20020201)41:3<390::AID-ANIE390>3.0.CO;2-B)
- Carlsson, P., & Kjellén, L. (2012). Heparin Biosynthesis. In R. Lever, B. Mulloy, & C. P. Page (Eds.), *Heparin—A Century of Progress* (Vol. 207, pp. 23–41). Springer Berlin Heidelberg. https://doi.org/10.1007/978-3-642-23056-1_2

- Castellot, J. J., Addonizio, M. L., Rosenberg, R., & Karnovsky, M. J. (1981). Cultured Endothelial Cells Produce a Heparinlike Inhibitor of Smooth Muscle Cell Growth. *The Journal of Cell Biology*, *90*(2), 372–379. JSTOR.
- Chen, X., Xiao, W., Qu, X., & Zhou, S. (2008). The Effect of Dalteparin, a Kind of Low Molecular Weight Heparin, on Lung Adenocarcinoma A549 Cell Line In Vitro. *Cancer Investigation*, *26*(7), 718–724.
<https://doi.org/10.1080/07357900801935631>
- Cheng, T.-Y. D., Cramb, S. M., Baade, P. D., Youlden, D. R., Nwogu, C., & Reid, M. E. (2016). The International Epidemiology of Lung Cancer: Latest Trends, Disparities, and Tumor Characteristics. *Journal of Thoracic Oncology : Official Publication of the International Association for the Study of Lung Cancer*, *11*(10), 1653–1671. <https://doi.org/10.1016/j.jtho.2016.05.021>
- Daley, W. P., Peters, S. B., & Larsen, M. (2008). Extracellular matrix dynamics in development and regenerative medicine. *Journal of Cell Science*, *121*(3), 255–264. <https://doi.org/10.1242/jcs.006064>
- Daouk, R., Hassane, M., Bahmad, H. F., Sinjab, A., Fujimoto, J., Abou-Kheir, W., & Kadara, H. (2019). Genome-Wide and Phenotypic Evaluation of Stem Cell Progenitors Derived From Gprc5a-Deficient Murine Lung Adenocarcinoma With Somatic Kras Mutations. *Frontiers in Oncology*, *9*.
<https://doi.org/10.3389/fonc.2019.00207>
- DeQuach, J. A., Mezzano, V., Miglani, A., Lange, S., Keller, G. M., Sheikh, F., & Christman, K. L. (2010). Simple and High Yielding Method for Preparing

- Tissue Specific Extracellular Matrix Coatings for Cell Culture. *PLoS ONE*, 5(9).
<https://doi.org/10.1371/journal.pone.0013039>
- Derby, M. A. (1978). Analysis of glycosaminoglycans within the extracellular environments encountered by migrating neural crest cells. *Developmental Biology*, 66(2), 321–336. [https://doi.org/10.1016/0012-1606\(78\)90241-5](https://doi.org/10.1016/0012-1606(78)90241-5)
- Eiselt, P., Yeh, J., Latvala, R. K., Shea, L. D., & Mooney, D. J. (2000). Porous carriers for biomedical applications based on alginate hydrogels. *Biomaterials*, 21(19), 1921–1927. [https://doi.org/10.1016/S0142-9612\(00\)00033-8](https://doi.org/10.1016/S0142-9612(00)00033-8)
- Engbring, J. A., & Kleinman, H. K. (2003). The basement membrane matrix in malignancy. *The Journal of Pathology*, 200(4), 465–470.
<https://doi.org/10.1002/path.1396>
- Eramo, A., Lotti, F., Sette, G., Piloizzi, E., Biffoni, M., Di Virgilio, A., Conticello, C., Ruco, L., Peschle, C., & De Maria, R. (2008). Identification and expansion of the tumorigenic lung cancer stem cell population. *Cell Death and Differentiation; Rome*, 15(3), 504–514.
<http://dx.doi.org.ezproxy.aub.edu.lb/10.1038/sj.cdd.4402283>
- Esquivel, C. O., Bergqvist, D., Björck, C.-G., & Nilsson, B. (1982). Comparison between commercial heparin, low molecular weight heparin and pentosan polysulfate on hemostasis and platelets in vivo. *Thrombosis Research*, 28(3), 389–399. [https://doi.org/10.1016/0049-3848\(82\)90120-7](https://doi.org/10.1016/0049-3848(82)90120-7)
- Faham, S., Linhardt, R. J., & Rees, D. C. (1998). Diversity does make a difference: Fibroblast growth factor-heparin interactions. *CURRENT OPINION IN STRUCTURAL BIOLOGY*, 8(5), 578–586.

- Fan, L., Jiang, L., Xu, Y., Zhou, Y., Shen, Y., Xie, W., Long, Z., & Zhou, J. (2011a). Synthesis and anticoagulant activity of sodium alginate sulfates. *Carbohydrate Polymers*, 83(4), 1797–1803. <https://doi.org/10.1016/j.carbpol.2010.10.038>
- Fan, L., Jiang, L., Xu, Y., Zhou, Y., Shen, Y., Xie, W., Long, Z., & Zhou, J. (2011b). Synthesis and anticoagulant activity of sodium alginate sulfates. *Carbohydrate Polymers*, 83(4), 1797–1803. <https://doi.org/10.1016/j.carbpol.2010.10.038>
- Farndale, R., Buttle, D., & Barrett, A. (1986). Improved quantitation and discrimination of sulphated glycosaminoglycans by use of dimethylmethylene blue. *Biochimica et Biophysica Acta (BBA) - General Subjects*, 883(2), 173–177. [https://doi.org/10.1016/0304-4165\(86\)90306-5](https://doi.org/10.1016/0304-4165(86)90306-5)
- Farndale, R. W., Sayers, C. A., & Barrett, A. J. (1982). A Direct Spectrophotometric Microassay for Sulfated Glycosaminoglycans in Cartilage Cultures. *Connective Tissue Research*, 9(4), 247–248. <https://doi.org/10.3109/03008208209160269>
- Frantz, C., Stewart, K. M., & Weaver, V. M. (2010). The extracellular matrix at a glance. *Journal of Cell Science*, 123(24), 4195–4200. <https://doi.org/10.1242/jcs.023820>
- Freeman, I., & Cohen, S. (2009). The influence of the sequential delivery of angiogenic factors from affinity-binding alginate scaffolds on vascularization. *Biomaterials*, 30(11), 2122–2131. <https://doi.org/10.1016/j.biomaterials.2008.12.057>
- Freeman, I., Kedem, A., & Cohen, S. (2008a). The effect of sulfation of alginate hydrogels on the specific binding and controlled release of heparin-binding proteins. *Biomaterials*, 29(22), 3260–3268. <https://doi.org/10.1016/j.biomaterials.2008.04.025>

- Freeman, I., Kedem, A., & Cohen, S. (2008b). The effect of sulfation of alginate hydrogels on the specific binding and controlled release of heparin-binding proteins. *Biomaterials*, *29*(22), 3260–3268.
<https://doi.org/10.1016/j.biomaterials.2008.04.025>
- Fujimoto, J., Kadara, H., Men, T., van Pelt, C., Lotan, D., & Lotan, R. (2010). Comparative Functional Genomics Analysis of NNK Tobacco-Carcinogen Induced Lung Adenocarcinoma Development in Gprc5a-Knockout Mice. *PLoS ONE*, *5*(7). <https://doi.org/10.1371/journal.pone.0011847>
- Fujimoto, J., Nunomura-Nakamura, S., Liu, Y., Lang, W., McDowell, T., Jakubek, Y., Ezzeddine, D., Ochieng, J. K., Petersen, J., Davies, G., Fukuoka, J., Wistuba, I. I., Ehli, E., Fowler, J., Scheet, P., & Kadara, H. (2017). Development of Kras mutant lung adenocarcinoma in mice with knockout of the airway lineage-specific gene Gprc5a. *International Journal of Cancer*, *141*(8), 1589–1599.
<https://doi.org/10.1002/ijc.30851>
- Gebäck, T., Schulz, M. M. P., Koumoutsakos, P., & Detmar, M. (2009). TScratch: A novel and simple software tool for automated analysis of monolayer wound healing assays. *BioTechniques*, *46*(4), 265–274.
<https://doi.org/10.2144/000113083>
- Gong, H., Sun, L., Chen, B., Han, Y., Pang, J., Wu, W., Qi, R., & Zhang, T. (2016). Evaluation of candidate reference genes for RT-qPCR studies in three metabolism related tissues of mice after caloric restriction. *Scientific Reports (Nature Publisher Group); London*, *6*, 38513.
<http://dx.doi.org.ezproxy.aub.edu.lb/10.1038/srep38513>

- Hardavella, G., George, R., & Sethi, T. (2016). Lung cancer stem cells—
Characteristics, phenotype. *Translational Lung Cancer Research*, 5(3), 272–279.
<https://doi.org/10.21037/tlcr.2016.02.01>
- Hejna, M., Raderer, M., & Zielinski, C. C. (1999). Inhibition of Metastases by
Anticoagulants. *JNCI Journal of the National Cancer Institute*, 91(1), 22–36.
<https://doi.org/10.1093/jnci/91.1.22>
- Ho, M. M., Ng, A. V., Lam, S., & Hung, J. Y. (2007). Side Population in Human Lung
Cancer Cell Lines and Tumors Is Enriched with Stem-like Cancer Cells. *Cancer
Research*, 67(10), 4827–4833. <https://doi.org/10.1158/0008-5472.CAN-06-3557>
- Holland, J. D., Klaus, A., Garratt, A. N., & Birchmeier, W. (2013). Wnt signaling in
stem and cancer stem cells. *Current Opinion in Cell Biology*, 25(2), 254–264.
<https://doi.org/10.1016/j.ceb.2013.01.004>
- Hoppensteadt, D., Chaudhry, A., Gray, A., Hejna, M., & Fareed, J. (2012). Effect of
Heparin and Its Derivatives On the Progression of Tumor Growth in Mouse
Lewis Lung Carcinoma Model. *Blood*, 120(21), 2274–2274.
<https://doi.org/10.1182/blood.V120.21.2274.2274>
- Houghton, J., Morozov, A., Smirnova, I., & Wang, T. C. (2007). Stem cells and cancer.
Seminars in Cancer Biology, 17(3), 191–203.
<https://doi.org/10.1016/j.semcancer.2006.04.003>
- Huang, E. H., Hynes, M. J., Zhang, T., Ginestier, C., Dontu, G., Appelman, H., Fields,
J. Z., Wicha, M. S., & Boman, B. M. (2009). Aldehyde Dehydrogenase 1 Is a
Marker for Normal and Malignant Human Colonic Stem Cells (SC) and Tracks

- SC Overpopulation during Colon Tumorigenesis. *Cancer Research*, 69(8), 3382–3389. <https://doi.org/10.1158/0008-5472.CAN-08-4418>
- Jackson, E. L. (2001). Analysis of lung tumor initiation and progression using conditional expression of oncogenic K-ras. *Genes & Development*, 15(24), 3243–3248. <https://doi.org/10.1101/gad.943001>
- Jackson, R. L., Busch, S. J., & Cardin, A. D. (1991). Glycosaminoglycans: Molecular properties, protein interactions, and role in physiological processes. *Physiological Reviews*, 71(2), 481–539. <https://doi.org/10.1152/physrev.1991.71.2.481>
- Jacobs-Tulleneers-Thevissen, D., Chintinne, M., Ling, Z., Gillard, P., Schoonjans, L., Delvaux, G., Strand, B. L., Gorus, F., Keymeulen, B., Pipeleers, D., & on behalf of the Beta Cell Therapy Consortium EU-FP7. (2013). Sustained function of alginate-encapsulated human islet cell implants in the peritoneal cavity of mice leading to a pilot study in a type 1 diabetic patient. *Diabetologia*, 56(7), 1605–1614. <https://doi.org/10.1007/s00125-013-2906-0>
- Jančík, S., Drábek, J., Radzioch, D., & Hajdúch, M. (2010). Clinical Relevance of KRAS in Human Cancers. *Journal of Biomedicine and Biotechnology*, 2010. <https://doi.org/10.1155/2010/150960>
- Järveläinen, H., Sainio, A., Koulu, M., Wight, T. N., & Penttinen, R. (2009). Extracellular Matrix Molecules: Potential Targets in Pharmacotherapy. *Pharmacological Reviews*, 61(2), 198–223. <https://doi.org/10.1124/pr.109.001289>

- Jiang, F., Qiu, Q., Khanna, A., Todd, N. W., Deepak, J., Xing, L., Wang, H., Liu, Z., Su, Y., Stass, S. A., & Katz, R. L. (2009). Aldehyde Dehydrogenase 1 Is a Tumor Stem Cell-Associated Marker in Lung Cancer. *Molecular Cancer Research*, 7(3), 330–338. <https://doi.org/10.1158/1541-7786.MCR-08-0393>
- Kadara, H., Kabbout, M., & Wistuba, I. I. (2012). Pulmonary adenocarcinoma: A renewed entity in 2011. *Respirology*, 17(1), 50–65. <https://doi.org/10.1111/j.1440-1843.2011.02095.x>
- Kadara, H., Scheet, P., Wistuba, I. I., & Spira, A. E. (2016). Early Events in the Molecular Pathogenesis of Lung Cancer. *Cancer Prevention Research*, 9(7), 518–527. <https://doi.org/10.1158/1940-6207.CAPR-15-0400>
- Kerschenmeyer, A., Arlov, Ø., Malheiro, V., Steinwachs, M., Rottmar, M., Maniura-Weber, K., Palazzolo, G., & Zenobi-Wong, M. (2017). Anti-oxidant and immune-modulatory properties of sulfated alginate derivatives on human chondrocytes and macrophages. *Biomaterials Science*, 5(9), 1756–1765. <https://doi.org/10.1039/C7BM00341B>
- Kim, C. F. B., Jackson, E. L., Woolfenden, A. E., Lawrence, S., Babar, I., Vogel, S., Crowley, D., Bronson, R. T., & Jacks, T. (2005). Identification of Bronchioalveolar Stem Cells in Normal Lung and Lung Cancer. *Cell*, 121(6), 823–835. <https://doi.org/10.1016/j.cell.2005.03.032>
- Kim, E., Kang, J., Cho, M., Lee, S., Seo, E., Choi, H., Kim, Y., Kim, J., Kang, K. Y., Kim, K. P., Han, J., Sheen, Y., Yum, Y. N., Park, S.-N., & Yoon, D.-Y. (2008). Profiling of transcripts and proteins modulated by the E7 oncogene in the lung

- tissue of E7-Tg mice by the omics approach. *Molecular Medicine Reports*, 2(1), 129–137. https://doi.org/10.3892/mmr_00000073
- Kjellén, L., Oldberg, Å., Rubin, K., & Höök, M. (1977). Binding of heparin and heparan sulphate to rat liver cells. *Biochemical and Biophysical Research Communications*, 74(1), 126–133. [https://doi.org/10.1016/0006-291X\(77\)91384-5](https://doi.org/10.1016/0006-291X(77)91384-5)
- Kleinman, H. K., & Martin, G. R. (2005). Matrigel: Basement membrane matrix with biological activity. *Seminars in Cancer Biology*, 15(5), 378–386. <https://doi.org/10.1016/j.semcancer.2005.05.004>
- Lai, J., Chien, J., Staub, J., Avula, R., Greene, E. L., Matthews, T. A., Smith, D. I., Kaufmann, S. H., Roberts, L. R., & Shridhar, V. (2003). Loss of HSulf-1 Up-regulates Heparin-binding Growth Factor Signaling in Cancer. *Journal of Biological Chemistry*, 278(25), 23107–23117. <https://doi.org/10.1074/jbc.M302203200>
- Lazo-Langner, A., Goss, G. D., Spaans, J. N., & Rodger, M. A. (2007). The effect of low-molecular-weight heparin on cancer survival. A systematic review and meta-analysis of randomized trials. *Journal of Thrombosis and Haemostasis*, 5(4), 729–737. <https://doi.org/10.1111/j.1538-7836.2007.02427.x>
- Lee, K. Y., & Mooney, D. J. (2012). Alginate: Properties and biomedical applications. *Progress in Polymer Science*, 37(1), 106–126. <https://doi.org/10.1016/j.progpolymsci.2011.06.003>

- Lemma, S., Avnet, S., Salerno, M., Chano, T., & Baldini, N. (2016). Identification and Validation of Housekeeping Genes for Gene Expression Analysis of Cancer Stem Cells. *PLoS ONE*, *11*(2). <https://doi.org/10.1371/journal.pone.0149481>
- Leung, E. L.-H., Fiscus, R. R., Tung, J. W., Tin, V. P.-C., Cheng, L. C., Sihoe, A. D.-L., Fink, L. M., Ma, Y., & Wong, M. P. (2010). Non-Small Cell Lung Cancer Cells Expressing CD44 Are Enriched for Stem Cell-Like Properties. *PLoS One; San Francisco*, *5*(11), e14062.
<http://dx.doi.org.ezproxy.aub.edu.lb/10.1371/journal.pone.0014062>
- Levi, B. P., Yilmaz, Ö. H., Duester, G., & Morrison, S. J. (2009). Aldehyde dehydrogenase 1a1 is dispensable for stem cell function in the mouse hematopoietic and nervous systems. *Blood*, *113*(8), 1670–1680.
<https://doi.org/10.1182/blood-2008-05-156752>
- Lindeman, N. I., Cagle, P. T., Beasley, M. B., Chitale, D. A., Dacic, S., Giaccone, G., Jenkins, R. B., Kwiatkowski, D. J., Saldivar, J.-S., Squire, J., Thunnissen, E., & Ladanyi, M. (2013). Molecular Testing Guideline for Selection of Lung Cancer Patients for EGFR and ALK Tyrosine Kinase Inhibitors: Guideline from the College of American Pathologists, International Association for the Study of Lung Cancer, and Association for Molecular Pathology. *Journal of Thoracic Oncology*, *8*(7), 823–859. <https://doi.org/10.1097/JTO.0b013e318290868f>
- Liu, J., Xiao, Z., Wong, S. K.-M., Tin, V. P.-C., Ho, K.-Y., Wang, J., Sham, M.-H., & Wong, M. P. (2013). Lung cancer tumorigenicity and drug resistance are maintained through ALDH^{hi}CD44^{hi} tumor initiating cells. *Oncotarget*, *4*(10), 1698–1711.

- Luan, L., Patil, N. K., Guo, Y., Hernandez, A., Bohannon, J. K., Fensterheim, B. A., Wang, J., Xu, Y., Enkhbaatar, P., Stark, R., & Sherwood, E. R. (2017). Comparative Transcriptome Profiles of Human Blood in Response to the Toll-like Receptor 4 Ligands Lipopolysaccharide and Monophosphoryl Lipid A. *Scientific Reports (Nature Publisher Group); London, 7*, 40050. <http://dx.doi.org.ezproxy.aub.edu.lb/10.1038/srep40050>
- Ma, L., Cheng, C., Nie, C., He, C., Deng, J., Wang, L., Xia, Y., & Zhao, C. (2016). Anticoagulant sodium alginate sulfates and their mussel-inspired heparin-mimetic coatings. *Journal of Materials Chemistry B, 4*(19), 3203–3215. <https://doi.org/10.1039/C6TB00636A>
- Mainardi, S., Mijimolle, N., Francoz, S., Vicente-Dueñas, C., Sánchez-García, I., & Barbacid, M. (2014). Identification of cancer initiating cells in K-Ras driven lung adenocarcinoma. *Proceedings of the National Academy of Sciences of the United States of America, 111*(1), 255–260. <https://doi.org/10.1073/pnas.1320383110>
- Marcum, J. A., McKenney, J. B., Galli, S. J., Jackman, R. W., & Rosenberg, R. D. (1986). Anticoagulant active heparin-like molecules from mast cell-deficient mice. *American Journal of Physiology-Heart and Circulatory Physiology, 250*(5), H879–H888. <https://doi.org/10.1152/ajpheart.1986.250.5.H879>
- Marks, J. L., Broderick, S., Zhou, Q., Chitale, D., Li, A. R., Zakowski, M. F., Kris, M. G., Rusch, V. W., Azzoli, C. G., Seshan, V. E., Ladanyi, M., & Pao, W. (2008). Prognostic and Therapeutic Implications of EGFR and KRAS Mutations in

- Resected Lung Adenocarcinoma. *Journal of Thoracic Oncology*, 3(2), 111–116.
<https://doi.org/10.1097/JTO.0b013e318160c607>
- Markstedt, K., Mantas, A., Tournier, I., Martínez Ávila, H., Hägg, D., & Gatenholm, P. (2015). 3D Bioprinting Human Chondrocytes with Nanocellulose–Alginate Bioink for Cartilage Tissue Engineering Applications. *Biomacromolecules*, 16(5), 1489–1496. <https://doi.org/10.1021/acs.biomac.5b00188>
- Meer, J.-Y. van der, Kellenbach, E., & Bos, L. J. van den. (2017). From Farm to Pharma: An Overview of Industrial Heparin Manufacturing Methods. *Molecules; Basel*, 22(6), 1025.
<http://dx.doi.org.ezproxy.aub.edu.lb/10.3390/molecules22061025>
- Meng, D., Yuan, M., Li, X., Chen, L., Yang, J., Zhao, X., Ma, W., & Xin, J. (2013). Prognostic value of K-RAS mutations in patients with non-small cell lung cancer: A systematic review with meta-analysis. *Lung Cancer*, 81(1), 1–10.
<https://doi.org/10.1016/j.lungcan.2013.03.019>
- Mhanna, R., Becher, J., Schnabelrauch, M., Reis, R. L., & Pashkuleva, I. (2017). Sulfated Alginate as a Mimic of Sulfated Glycosaminoglycans: Binding of Growth Factors and Effect on Stem Cell Behavior. *Advanced Biosystems*, 1(7), 1700043. <https://doi.org/10.1002/adbi.201700043>
- Mhanna, R., Kashyap, A., Palazzolo, G., Vallmajo-Martin, Q., Becher, J., Möller, S., Schnabelrauch, M., & Zenobi-Wong, M. (2013). Chondrocyte Culture in Three Dimensional Alginate Sulfate Hydrogels Promotes Proliferation While Maintaining Expression of Chondrogenic Markers. *Tissue Engineering Part A*, 20(9–10), 1454–1464. <https://doi.org/10.1089/ten.tea.2013.0544>

- Mhanna, R., Kashyap, A., Palazzolo, G., Vallmajo-Martin, Q., Becher, J., Möller, S., Schnabelrauch, M., & Zenobi-Wong, M. (2014). Chondrocyte Culture in Three Dimensional Alginate Sulfate Hydrogels Promotes Proliferation While Maintaining Expression of Chondrogenic Markers. *Tissue Engineering. Part A*, 20(9–10), 1454–1464. <https://doi.org/10.1089/ten.tea.2013.0544>
- Miyaji, H., & Misaki, A. (1973). Distribution of Sulfate Groups in the Partially Sulfated Dextrans. *The Journal of Biochemistry*, 74(6), 1131–1139. <https://doi.org/10.1093/oxfordjournals.jbchem.a130340>
- Msheik, H., Azar, J., El Sabeh, M., Abou-Kheir, W., & Daoud, G. (2020). HTR-8/SVneo: A model for epithelial to mesenchymal transition in the human placenta. *Placenta*, 90, 90–97. <https://doi.org/10.1016/j.placenta.2019.12.013>
- Müller, M., Öztürk, E., Arlov, Ø., Gatenholm, P., & Zenobi-Wong, M. (2017). Alginate Sulfate–Nanocellulose Bioinks for Cartilage Bioprinting Applications. *Annals of Biomedical Engineering*, 45(1), 210–223. <https://doi.org/10.1007/s10439-016-1704-5>
- Niu, Q., Wang, W., Li, Y., Ruden, D. M., Wang, F., Li, Y., Wang, F., Song, J., & Zheng, K. (2012). Low Molecular Weight Heparin Ablates Lung Cancer Cisplatin-Resistance by Inducing Proteasome-Mediated ABCG2 Protein Degradation. *PLoS ONE*, 7(7), e41035. <https://doi.org/10.1371/journal.pone.0041035>
- Pacheco-Pinedo, E. C., Durham, A. C., Stewart, K. M., Goss, A. M., Lu, M. M., DeMayo, F. J., & Morrisey, E. E. (2011). Wnt/[Beta]-catenin signaling accelerates mouse lung tumorigenesis by imposing an embryonic distal

- progenitor phenotype on lung epithelium. *Journal of Clinical Investigation; Ann Arbor*, 121(5), 1935–1945.
- Papakonstantinou, E., & Karakiulakis, G. (2009). The ‘sweet’ and ‘bitter’ involvement of glycosaminoglycans in lung diseases: Pharmacotherapeutic relevance. *British Journal of Pharmacology*, 157(7), 1111–1127. <https://doi.org/10.1111/j.1476-5381.2009.00279.x>
- Park, Kwon-sik, Martelotto, L. G., Peifer, M., Sos, M. L., Karnezis, A. N., Mahjoub, M. R., Bernard, K., Conklin, J. F., Szczepny, A., Yuan, J., Guo, R., Ospina, B., Falzon, J., Bennett, S., Brown, T. J., Markovic, A., Devereux, W. L., Ocasio, C. A., Chen, J. K., ... Sage, J. (2011). A crucial requirement for Hedgehog signaling in small cell lung cancer. *Nature Medicine; New York*, 17(11), 1504–1508. <http://dx.doi.org.ezproxy.aub.edu.lb/10.1038/nm.2473>
- Park, Kyeongsoon, Kim, Y., Lee, G. Y., Park, R., Kim, I., Kim, S. Y., & Byun, Y. (2008). Tumor Endothelial Cell Targeted Cyclic RGD-modified Heparin Derivative: Inhibition of Angiogenesis and Tumor Growth. *Pharmaceutical Research; New York*, 25(12), 2786–2798. <http://dx.doi.org.ezproxy.aub.edu.lb/10.1007/s11095-008-9643-y>
- Patin, E. C., Soulard, D., Fleury, S., Hassane, M., Dombrowicz, D., Faveeuw, C., Trottein, F., & Paget, C. (2018). Type I IFN Receptor Signaling Controls IL7-Dependent Accumulation and Activity of Protumoral IL17A-Producing $\gamma\delta$ T Cells in Breast Cancer. *Cancer Research*, 78(1), 195–204. <https://doi.org/10.1158/0008-5472.CAN-17-1416>

- Pawar, S. N., & Edgar, K. J. (2012). Alginate derivatization: A review of chemistry, properties and applications. *Biomaterials*, 33(11), 3279–3305.
<https://doi.org/10.1016/j.biomaterials.2012.01.007>
- Pelosi, P., Rocco, P. R. M., Negrini, D., & Passi, A. (2007). The extracellular matrix of the lung and its role in edema formation. *Anais Da Academia Brasileira de Ciências*, 79(2), 285–297. <https://doi.org/10.1590/S0001-37652007000200010>
- Peng, X.-H., Wang, Y., Huang, D., Wang, Y., Shin, H. J., Chen, Z., Spewak, M. B., Mao, H., Wang, X., Wang, Y., Chen, Z. (Georgia), Nie, S., & Shin, D. M. (2011). Targeted Delivery of Cisplatin to Lung Cancer Using ScFvEGFR-Heparin-Cisplatin Nanoparticles. *ACS Nano*, 5(12), 9480–9493.
<https://doi.org/10.1021/nm202410f>
- Pine, S. R., Marshall, B., & Varticovski, L. (2008). Lung Cancer Stem Cells. *Disease Markers*, 24(4–5), 257–266. <https://doi.org/10.1155/2008/396281>
- Rehm, B. H. A., & Valla, S. (1997). Bacterial alginates: Biosynthesis and applications. *Applied Microbiology and Biotechnology*, 48(3), 281–288.
<https://doi.org/10.1007/s002530051051>
- Riely, G. J., Marks, J., & Pao, W. (2009). KRAS Mutations in Non–Small Cell Lung Cancer. *Proceedings of the American Thoracic Society*, 6(2), 201–205.
<https://doi.org/10.1513/pats.200809-107LC>
- Rock, J. R., & Hogan, B. L. M. (2011). Epithelial Progenitor Cells in Lung Development, Maintenance, Repair, and Disease. *Annual Review of Cell and Developmental Biology*, 27(1), 493–512. <https://doi.org/10.1146/annurev-cellbio-100109-104040>

- Ronghua, H., Yumin, D., & Jianhong, Y. (2003a). Preparation and in vitro anticoagulant activities of alginate sulfate and its quaterized derivatives. *Carbohydrate Polymers*, 52(1), 19–24. [https://doi.org/10.1016/S0144-8617\(02\)00258-8](https://doi.org/10.1016/S0144-8617(02)00258-8)
- Ronghua, H., Yumin, D., & Jianhong, Y. (2003b). Preparation and in vitro anticoagulant activities of alginate sulfate and its quaterized derivatives. *Carbohydrate Polymers*, 52(1), 19–24. [https://doi.org/10.1016/S0144-8617\(02\)00258-8](https://doi.org/10.1016/S0144-8617(02)00258-8)
- Ruvinov, E., Freeman, I., Fredo, R., & Cohen, S. (2016). Spontaneous Coassembly of Biologically Active Nanoparticles via Affinity Binding of Heparin-Binding Proteins to Alginate-Sulfate. *Nano Letters*, 16(2), 883–888. <https://doi.org/10.1021/acs.nanolett.5b03598>
- Ruvinov, E., Leor, J., & Cohen, S. (2010). The effects of controlled HGF delivery from an affinity-binding alginate biomaterial on angiogenesis and blood perfusion in a hindlimb ischemia model. *Biomaterials*, 31(16), 4573–4582. <https://doi.org/10.1016/j.biomaterials.2010.02.026>
- Salnikov, A. V., Gladkikh, J., Moldenhauer, G., Volm, M., Mattern, J., & Herr, I. (2010). CD133 is indicative for a resistance phenotype but does not represent a prognostic marker for survival of non-small cell lung cancer patients. *International Journal of Cancer*, 126(4), 950–958. <https://doi.org/10.1002/ijc.24822>
- Sasisekharan, R., & Venkataraman, G. (2000). Heparin and heparan sulfate: Biosynthesis, structure and function. *Current Opinion in Chemical Biology*, 4(6), 626–631. [https://doi.org/10.1016/S1367-5931\(00\)00145-9](https://doi.org/10.1016/S1367-5931(00)00145-9)

- Sato, T., Shibata, W., Hikiba, Y., Kaneta, Y., Suzuki, N., Ihara, S., Ishii, Y., Sue, S., Kameta, E., Sugimori, M., Yamada, H., Kaneko, H., Sasaki, T., Ishii, T., Tamura, T., Kondo, M., & Maeda, S. (2017). C-Jun N-terminal kinase in pancreatic tumor stroma augments tumor development in mice. *Cancer Science*, *108*(11), 2156–2165. <https://doi.org/10.1111/cas.13382>
- Sha, H., Yang, L., Liu, M., Xia, S., Liu, Y., Liu, F., Kersten, S., & Qi, L. (2014). Adipocyte Spliced Form of X-Box–Binding Protein 1 Promotes Adiponectin Multimerization and Systemic Glucose Homeostasis. *Diabetes*, *63*(3), 867–879. <https://doi.org/10.2337/db13-1067>
- Siegel, R. L., Miller, K. D., & Jemal, A. (2019, January 1). *Cancer statistics, 2019*. CA: A Cancer Journal for Clinicians. <https://doi.org/10.3322/caac.21551>
- Skoulidis, F., Albacker, L., Hellmann, M., Awad, M., Gainor, J., Goldberg, M., Schrock, A., Gay, L., Elvin, J., Ross, J., Rizvi, H., Carter, B., Erasmus, J., Halpenny, D., Plodkowski, A., Long, N., Nishino-Habatu, M., Denning, W., Rodriguez-Canales, J., ... Heymach, J. (2017). MA 05.02 STK11/LKB1 Loss of Function Genomic Alterations Predict Primary Resistance to PD-1/PD-L1 Axis Blockade in KRAS-Mutant NSCLC. *Journal of Thoracic Oncology*, *12*(11, Supplement 2), S1815. <https://doi.org/10.1016/j.jtho.2017.09.479>
- Skoulidis, Ferdinandos, Byers, L. A., Diao, L., Papadimitrakopoulou, V. A., Tong, P., Izzo, J., Behrens, C., Kadara, H., Parra, E. R., Canales, J. R., Zhang, J., Giri, U., Gudikote, J., Cortez, M. A., Yang, C., Fan, Y., Peyton, M., Girard, L., Coombes, K. R., ... Heymach, J. V. (2015). Co-occurring Genomic Alterations Define Major Subsets of KRAS-Mutant Lung Adenocarcinoma with Distinct Biology,

- Immune Profiles, and Therapeutic Vulnerabilities. *Cancer Discovery*, 5(8), 860–877. <https://doi.org/10.1158/2159-8290.CD-14-1236>
- Smidsrød, O., & Skjåk-Bræk, G. (1990). Alginate as immobilization matrix for cells. *Trends in Biotechnology*, 8, 71–78. [https://doi.org/10.1016/0167-7799\(90\)90139-O](https://doi.org/10.1016/0167-7799(90)90139-O)
- Sullivan, J. P., Spinola, M., Dodge, M., Raso, M. G., Behrens, C., Gao, B., Schuster, K., Shao, C., Larsen, J. E., Sullivan, L. A., Honorio, S., Xie, Y., Scaglioni, P. P., DiMaio, J. M., Gazdar, A. F., Shay, J. W., Wistuba, I. I., & Minna, J. D. (2010). Aldehyde Dehydrogenase Activity Selects for Lung Adenocarcinoma Stem Cells Dependent on Notch Signaling. *Cancer Research*, 70(23), 9937–9948. <https://doi.org/10.1158/0008-5472.CAN-10-0881>
- Sun, S., Hu, Z., Huang, S., Ye, X., Wang, J., Chang, J., Wu, X., Wang, Q., Zhang, L., Hu, X., & Yu, H. (2019). REG4 is an indicator for KRAS mutant lung adenocarcinoma with TTF-1 low expression. *Journal of Cancer Research and Clinical Oncology*, 145(9), 2273–2283. <https://doi.org/10.1007/s00432-019-02988-y>
- Sutherland, K. D., & Berns, A. (2010). Cell of origin of lung cancer. *Molecular Oncology*, 4(5), 397–403. <https://doi.org/10.1016/j.molonc.2010.05.002>
- Sutherland, K. D., Song, J.-Y., Kwon, M. C., Proost, N., Zevenhoven, J., & Berns, A. (2014). Multiple cells-of-origin of mutant K-Ras-induced mouse lung adenocarcinoma. *Proceedings of the National Academy of Sciences*, 111(13), 4952–4957. <https://doi.org/10.1073/pnas.1319963111>

- Tachezy, M., Zander, H., Wolters-Eisfeld, G., Müller, J., Wicklein, D., Gebauer, F., Izbicki, J. R., & Bockhorn, M. (2014). Activated Leukocyte Cell Adhesion Molecule (CD166): An “Inert” Cancer Stem Cell Marker for Non-Small Cell Lung Cancer? *STEM CELLS*, 32(6), 1429–1436.
<https://doi.org/10.1002/stem.1665>
- Tønnesen, H. H., & Karlsen, J. (2002). Alginate in Drug Delivery Systems. *Drug Development and Industrial Pharmacy*, 28(6), 621–630.
<https://doi.org/10.1081/DDC-120003853>
- van Meerbeeck, J. P., Fennell, D. A., & De Ruyscher, D. K. (2011). Small-cell lung cancer. *The Lancet*, 378(9804), 1741–1755. [https://doi.org/10.1016/S0140-6736\(11\)60165-7](https://doi.org/10.1016/S0140-6736(11)60165-7)
- Vivès, R. R., Pye, D. A., Salmivirta, M., Hopwood, J. J., Lindahl, U., & Gallagher, J. T. (1999). Sequence analysis of heparan sulphate and heparin oligosaccharides. *The Biochemical Journal*, 339 (Pt 3), 767–773.
- Xu, X., Rock, J. R., Lu, Y., Futtner, C., Schwab, B., Guinney, J., Hogan, B. L. M., & Onaitis, M. W. (2012). Evidence for type II cells as cells of origin of K-Ras-induced distal lung adenocarcinoma. *Proceedings of the National Academy of Sciences*, 109(13), 4910–4915. <https://doi.org/10.1073/pnas.1112499109>
- Xu, Xiaolin, Zhu, X., Lu, W., He, Y., Wang, Y., & Liu, F. (2019). Effect of Sulfated Polysaccharide from *Undaria pinnatifida* (SPUP) on Proliferation, Migration, and Apoptosis of Human Prostatic Cancer. *International Journal of Polymer Science*, 2019, 1–7. <https://doi.org/10.1155/2019/7690764>

- Yu, M., Ji, Y., Qi, Z., Cui, D., Xin, G., Wang, B., Cao, Y., & Wang, D. (2017). Anti-tumor activity of sulfated polysaccharides from *Sargassum fusiforme*. *Saudi Pharmaceutical Journal : SPJ*, 25(4), 464–468.
<https://doi.org/10.1016/j.jsps.2017.04.007>
- Yu, Z., Pestell, T. G., Lisanti, M. P., & Pestell, R. G. (2012). Cancer stem cells. *The International Journal of Biochemistry & Cell Biology*, 44(12), 2144–2151.
<https://doi.org/10.1016/j.biocel.2012.08.022>
- Yung, S., & Chan, T. M. (2007a). Glycosaminoglycans and proteoglycans: Overlooked entities? *Peritoneal Dialysis International : Journal of the International Society for Peritoneal Dialysis*, 27(Suppl), NaN-NaN.
- Yung, S., & Chan, T. M. (2007b). Glycosaminoglycans and proteoglycans: Overlooked entities. *Peritoneal Dialysis International*, 104–109.
- Zappa, C., & Mousa, S. A. (2016). Non-small cell lung cancer: Current treatment and future advances. *Translational Lung Cancer Research*, 5(3), 288–300.
<https://doi.org/10.21037/tlcr.2016.06.07>
- Zhang, N., Lou, W., Ji, F., Qiu, L., Tsang, B. K., & Di, W. (2016). Low molecular weight heparin and cancer survival: Clinical trials and experimental mechanisms. *Journal of Cancer Research & Clinical Oncology; Heidelberg*, 142(8), 1807–1816. <http://dx.doi.org.ezproxy.aub.edu.lb/10.1007/s00432-016-2131-6>
- Zhao, X., Yu, G., Guan, H., Yue, N., Zhang, Z., & Li, H. (2007). Preparation of low-molecular-weight polyguluronate sulfate and its anticoagulant and anti-

inflammatory activities. *Carbohydrate Polymers*, 69(2), 272–279.

<https://doi.org/10.1016/j.carbpol.2006.10.024>